Results: The usefulness of the color and image quality evaluation slides was demonstrated. Furthermore, the new slide for Optics evaluation showed interesting results. Some system showed very good results in the Image Quality Evaluation and Color however, the result for the new slide was not good.

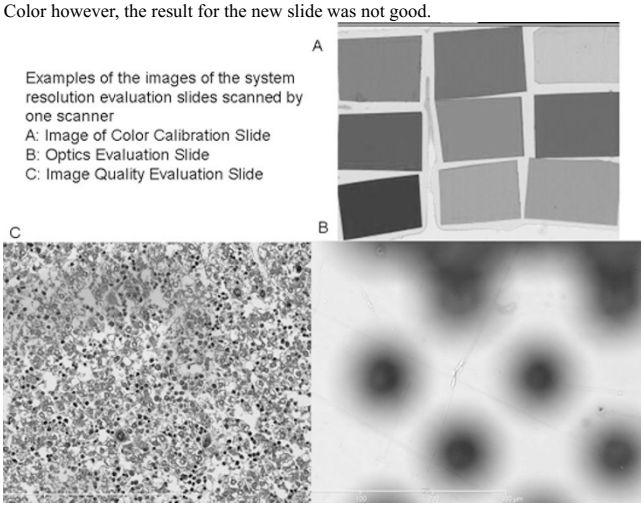

After the investigation of the system's component, we found that the system has relatively lower optics quality than image acquisition device If optics quality is improved, it is expected that the system resolution would also improve.

Conclusions: The importance of the additional slide to evaluate the optics of WSI from many aspects was demonstrated. The new slide could help improve system resolution of Whole Slide Imaging System toward Standardization.

Kidney

1651 Arhgap24 Downregulation Is Associated with Foot Process Effacement in Minimal Change Disease

S Akilesh, J Samuel, J Gaut, S Jain, A Shaw, H Liapis. Barnes-Jewish Hospital, St. Louis, MO; Washington University School of Medicine, St. Louis, MO.

Background: In vitro studies on glomerular epithelial cells (podocytes) suggest that increased membrane motility may contribute to foot process effacement and proteinuria. Recently, we identified Arhgap24, as a gene that suppresses membrane dynamics of podocytes in vitro. In human and murine kidney, podocytes normally express high levels of Arhgap24 protein, but the protein is susceptible to degradation. Therefore, we hypothesized that Arhgap24 levels would be reduced in proteinuric kidney diseases such as Minimal Change Disease (MCD) where foot process effacement is the key diagnostic feature.

Design: We developed new antibody reagents to stain for Arhgap24 and validated their specificity. Using these antibodies, in a proof of concept study, we stained fresh frozen normal kidney and biopsy material from a 10 year old boy with MCD (proven by electron microscopy). We examined the immunofluorescent staining intensity of Arhgap24 in podocytes in both samples.

Results: 1) Our newly developed antibodies stain Arhgap24 in human podocytes in fresh frozen kidney tissue (Figure 1, left panel).

2) Arhgap24 levels are decreased in a patient with minimal change disease (Figure 1, right panel).

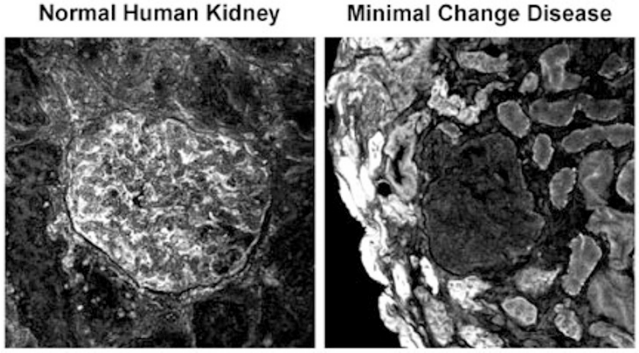

Conclusions: Our cell biological studies predicted that Arhgap24 downregulation would increase podocyte membrane motility in vitro and cause foot process effacement in vivo. Here we show, in a pilot study, that Arhgap24 expression is indeed decreased in a patient with diagnosed MCD, the prototypic kidney disease with foot process effacement. We are currently extending this study to additional patients and will also test the antibody reagents on FFPE kidney tissue. If successful, Arhgap24 downregulation would be a useful IHC marker of MCD when electron microscopy is not available. This study also shows how understanding of the cell biology of cultured podocytes can lead to a useful prediction of biologic behavior in patients.

1652 Renal Extramedullary Hematopoiesis Mimicking Tubulointerstitial Nephritis

MP Alexander, SH Nasr, PJ Kurtin, ME Fidler, LD Cornell. Mayo Clinic, Rochester, MN.

Background: Extramedullary hematopoiesis (EMH) is the presence and growth of hematopoietic tissue outside of the bone marrow, usually involving the liver and spleen. EMH of the kidney has rarely been reported. This is the first series outlining the clinicopathologic spectrum of intrarenal EMH.

Design: Patients (pts) with EMH in the kidney were identified from a biopsy database. Presenting clinical and laboratory findings and treatment and follow-up data were obtained. Pathology material was reviewed.

Results: Eight pts with intrarenal EMH were identified. The mean age at presentation was 68 yr (range 47-87); males predominated (M:F=7:1). All pts presented with renal failure, 2 with acute renal failure. The mean serum creatinine (SCr) at biopsy was 3.3 mg/dl (range 1.3-7.3). Six pts had proteinuria, 3 with nephrotic-range proteinuria. All biopsies showed a diffuse interstitial infiltrate that included megakaryocytes, granulocyte precursors (including many eosinophils) and clustered erythroid precursors, highlighted by immunostains for CD61, myeloperoxidase and glycophorin A. Tubular injury was present, but tubulitis was absent or rare. Two biopsies showed extrarenal extension. Two biopsies were misdiagnosed as tubulointerstitial nephritis (TIN). Five biopsies showed concurrent glomerular disease: 1 with fibrillary glomerulonephritis (GN) alone, 1 with fibrillary GN and chronic thrombotic microangiopathy (TMA), 1 with diabetic glomerulosclerosis and chronic TMA, and 2 with focal segmental glomerulosclerosis. All 8 pts had an underlying hematologic malignancy: 5, primary myelofibrosis; 2, an unclassifiable chronic myeloproliferative neoplasm (MPN); and 1, multiple myeloma (MM) with extensive bone marrow involvement. In 6 pts, the hematologic malignancy was diagnosed prior to renal biopsy by a mean of 78 mos (range 7-180); in 2 pts, renal EMH was the first manifestation of MPN or MM. Six pts also had EMH in the liver and/or spleen.

Clinical follow-up data were available in all pts, at a mean of 9.6 mos post-biopsy (range 1-23). Five pts were treated with hydroxyurea and/or other chemotherapy, 1 was treated with steroids, and treatment data were not available for 2 patients. The mean SCr at follow-up in 7 pts without end-stage renal disease (ESRD) was 1.8 mg/dl (range, 1.1-2.7). SCr improved in 2 pts to near-baseline; 5 had persistent renal dysfunction; and 1 progressed to ESRD within 3 mos.

Conclusions: EMH should be considered in the differential diagnosis of TIN, even in pts without a previously known hematologic malignancy. Intrarenal EMH may have associated glomerular disease. Treatment of the underlying malignancy may improve renal function.

1653 Membranous Glomerulonephritis Secondary to IgG4-Related Disease

MP Alexander, IW Gibson, Y Raissian, S Chari, N Takahashi, SH Nasr, S Sethi, TC Smyrk, LD Cornell. Mayo Clinic, Rochester, MN; University of Manitoba, Winnipeg, MB, Canada.

Background: IgG4-related disease (IgG4-RD) is a multiorgan inflammatory disease. Renal involvement is usually recognized in the form of IgG4-related tubulointerstitial nephritis (IgG4-TIN). There are case reports of glomerular disease associated with IgG4-RD, usually membranous glomerulonephritis (MGN). This is the first series of MGN associated with IgG4-RD.

Design: Patients(pts) were identified from a biopsy database based on the combination of MGN and clinical or histopathologic evidence of IgG4-TIN or other organ involvement by IgG4-RD. Presenting clinical data and treatment and follow-up data were obtained. Pathology material was reviewed.

Results: Eight IgG4-RD pts with MGN were identified. All pts had nephrotic-range proteinuria (ave 9.6 g/day;range 3.5-16). The mean serum creatinine (SCr) was 2.5 mg/dl(range 0.8-6.6); one pt had acute renal failure due to IgG4-TIN. 6 pts (75%) had other organ involvement by IgG4 disease. All 4 pts with available data had an increased serum IgG4 level. On biopsy, 4 pts (50%) had concurrent IgG4-TIN with increased IgG4+ plasma cells. Two pts had other glomerular disease in addition to MGN: one had diabetic glomerulosclerosis and the other had IgA nephropathy. One pt had a segmental endocapillary proliferative pattern with MGN. By immunofluorescence, glomeruli showed granular glomerular capillary loop staining for IgG, C3, kappa and lambda. One biopsy showed tubular basement membrane deposits. Electron microscopy revealed stage I-II MGN.

Follow-up data were available for all pts, at a mean of 37 mos(range 1-184). 6 of 8 pts were treated for MGN. Two pts received prednisone monotherapy, 2 prednisone followed by mycophenolate mofetil (MMF), one rituximab and MMF, and one prednisone and cyclophosphamide. The 2 untreated pts developed end-stage renal disease within 1 mo and 3 yrs; one of these pts was transplanted, without clinical evidence of recurrent disease and with stable SCr 11 years post-transplant. The mean SCr at follow-up of the other 6 pts was 1.4 mg/dl(range 0.8-2.5) and proteinuria was 1.4 g/day range 0.17-3.1). 2/6 pts showed a complete response of proteinuria to treatment and 3 showed a partial response; the other had heavy proteinuria at 1 mo follow-up. The pt with acute renal failure and TIN showed marked improvement in SCr with prednisone monotherapy.

Conclusions: MGN should be included in the spectrum of IgG4-RD and should be suspected in pts with nephrotic-range proteinuria. MGN can occur concomitantly with IgG4-TIN. Treatment with immunosuppressive drugs may improve proteinuria and may improve renal function in pts with decreased renal function.

1654 Clinico-Patholgical Findings in Iranian Elderly Kidney Patients – A Case Series Study

M Asgari, S Ossareh, S Savaj, E Abdi, Y Ataipour, T Malakoutian. Hasheminejad Clinical Research Developing Center (HCRDC), Tehran University of Medical Sciences (TUMS), Tehran, Islamic Republic of Iran; Firoozgar Hospital, Tehran University of Medical Sciences (TUMS), Tehran, Islamic Republic of Iran.

Background: Most of the renal lesions in the elderly are considered to be the result of aging but renal biopsies in the elderly show frequent finding of various renal pathologies, with some differences in distribution and clinical presentation compared to the younger patients. We planned this study to investigate the cause of renal biopsy and clinico-pathologic presentations of renal biopsy findings in the elderly patients in our center.

Design: Data from 2268 patients (56% male, mean age: 37.8+/- 16 years) between 1997 and 2011 were collected in questionnaires including demographic data, renal syndrome at presentation and laboratory findings. 182 Patients older than 64 years of age were defined as the elderly group.

Results: Elderly group showed the same distribution of renal biopsy findings of all patinets, however in this group amyloidosis, IgAN and diffuse crescentic GN, diabetic nephropathy and multiple myeloma were the most frequent diagnoses after MG and FSGS. There were higher prevalence of male patients ($p<0.004$), hypertension ($p<0.001$) and azotemia. Nephrotic syndrome was the most common renal syndrome in this group, as in the younger group. Secondary glomerular disease was seen in 26.9% of elderly with a lower risk of lupus nephritis and higher risk of amyloidosis, multiple myeloma, light chain deposition disease and hypertensive nephrosclerosis, compared to younger patients. In patients presented with nephrotic syndrome MG was the most common diagnosis found followed by amyloidosis, FSGS and membranoproliferative glomerulonephritis (MPGN).

Conclusions: Our study showed higher rate of renal biopsy done for older men (65.9%) and nephrotic syndrome was the most common reason for performing renal biopsy in the elderly patients (57.6%) that was similar to the patients <65y (57.4%). MG was the most frequent pathology in the elderly followed by FSGS and amyloidosis. In our study 8% of all renal biopsy cases are from elderly that is less than similar studies. This could be due to limitations on performing renal biopsy in this group. Although our study and others showed most of these diseases are treatable and biopsy indications of elderly patients need to be expanded in our center.

1655 Clinicopathologic Characterization of Membranous Glomerulonephritis with Crescents

C Barrett, D Houghton, M Troxell. OHSU, Portland, OR.

Background: Membranous glomerulonephritis (MGN) infrequently presents with glomerular crescents and necrosis (NCGN), except in lupus nephritis. This combination of glomerular lesions may represent a coincidental occurrence of two disease processes, or may be related to each other, or to a common pathophysiologic process. We reviewed our institution's experience with non-lupus MGN-NCGN, including IgG subclass staining, in order to further address this question.

Design: Renal biopsies with both MGN and NCGN were identified by searching the pathology database (2000-2011). Lupus nephritis cases were excluded, yielding 12 cases. Biopsy pathology was reviewed, and correlated with available patient history at presentation, treatment, and followup. In addition, immunofluorescent staining for IgG subclasses was performed on 6 cases with archival frozen tissue (antibodies from The Binding Site).

Results: MGN-NCGN was seen in biopsies from 2 children and 10 adults (6 patients >70 years old). ANCA serologies were positive in 7/10 patients (all MPO/P-ANCA); none had evidence of anti-GBM disease. ANA was positive in 5/10 patients, none with subsequent clinical evidence of lupus. Two patients had active malignancy (ovarian cancer, CLL, with CLL focally present in renal biopsy). One patient each had a history of treatment with hydralazine and gold (remote), and one reported infrequent NSAIDs use. Hepatitis serologies were negative in all cases with available data.

In MGN-NCGN biopsies, cellular or fibrocellular crescents were present in a mean of 26% of glomeruli (range 3-70%). Five biopsies had minor mesangial or endocapillary hypercellularity. Five of 12 cases had >50% interstitial fibrosis and tubular atrophy at biopsy. One biopsy had C3-only capillary wall deposits; none had immune deposits other than typical MGN pattern. Of six tested cases, 4 showed no IgG4 in the IgG deposits, while in 2 cases IgG4 staining was co-dominant with IgG1. IgG4 staining was negative in the patient with concurrent ovarian cancer.

Conclusions: Review of MGN-NCGN cases at our center revealed evidence of heterogeneous pathogenesis. A substantial subgroup of patients (7) was positive for MPO/P-ANCA, the majority of whom were negative for IgG4 (3 negative of 4 tested), a staining pattern not typical of idiopathic MGN. At least 2 patients were likely to have paraneoplastic MGN. Based on history of concurrent neoplasm, and/or lack of IgG4 staining, at least 5/12 cases of MGN-NCGN likely represent secondary MGN. This finding suggests that MGN and pauci-immune NCGN, when they coexist in a non-lupus patient, may relate to each other or to a common cause.

1656 The Effects of Oxidative Stress on Dendritic Cell Migration and T-Cell Interaction

I Batal, J Azzi, M Mounayar, B Mfarrej, R Abdi. Brigham and Women's Hospital, Boston, MA; Brigham and Women's, Boston, MA.

Background: In ischemia reperfusion injury (IRI), donor-derived dendritic cells (DDDCs) play a pivotal role in accelerating rejection. The specific mechanisms by which DDDCs increase allogenicity have not been systematically investigated.

Design: Bone marrow-derived dendritic cells (DCs) generated from C57BL/6 (B6) mice were utilized. H2O2, a well-accepted *In Vitro* model for IRI, was used to induce oxidative stress (OXS). H2O2-treated DCs (OXS-DCs) were compared to non-treated DCs (NT-DCs).

Results: The ability of DDDCs to mount rejection depends on their efficient migration. OXS-DCs upregulated CCR7, a specific receptor for CCL21 expressed on lymphatics and lymphoid tissues. Compared to NT-DCs, OXS-DCs revealed increased CCL21-induced Transwell migration (TWM) ($p=0.006$). This increased migration is dependent on OXS and protein synthesis because it was abrogated by pretreatment with Catalase and Cycloheximide. Furthermore, OXS-DCs showed pAKT and pNFKB activation. This prompted us to study the role of PI3Kγ and NF-KB in DCs migration. OXS-DCs from PI3Kγ-/- mice showed decreased TWM compared to OXS-DCs from wild-type ($p=0.04$). The latter also revealed decreased TWM when pretreated with NF-KB inhibitor ($p=0.004$).

Besides migration, DDDCs need to activate host T-cells to trigger rejection. Compared to NT-DCs, OXS-DCs upregulated CD80 and CD86 costimulatory receptors and increased allogeneic splenocyte proliferation measured by thymidine uptake. To explore whether this lymphocytic proliferation is cytotoxic vs. helper cell, we utilized transgenic OTI and OTII mice. TCR of these mice react specifically with OVA MHC-I and II restricted residues, respectively. DCs were incubated with OVA-restricted MHC-I and II and co-cultured with CD8+OTI and CD4+OTII cells, respectively. CD4+OTII incubated with OXS-DCs revealed increased proliferation assessed by CFSE ($p=0.02$) and IFN-G secretion assessed by ELISPOT ($p=0.009$) compared to these incubated with NT-DCs. The results for CD8+OTI were less significant. Finally, proinflammatory cytokines of DCs supernatant were measured by Luminex. OXS-DCs showed increased IL-6 secretion. T-regulatory (T-reg) cells were then assessed since IL-6 is a potential inhibitor of T-reg formation. In a fully allogeneic MLR, decreased CD4+ Treg:effector ratio was observed following incubation with OXS-DC compared to NT-DCs ($p<0.001$).

Conclusions: OXS increases DCs migration via PI3Kγ and NF-KB and alloactivation of effector but not T-reg CD4+ cells. These findings might help guiding future therapy to induce tolerance by targeting DDDCs.

1657 Infective Endocarditis-Associated Glomerulonephritis: A Report of 37 Cases

CL Boils, SH Nasr, PD Walker, CP Larsen. Nephropathology Associates, Little Rock, AR; Mayo Clinic, Rochester, MN.

Background: Endocarditis-associated glomerulonephritis was first described over a century ago, with most literature originating from autopsy specimens during the pre-antibiotic era. In order to better define the morphologic spectrum of this entity, we report the largest case series of infective endocarditis-associated glomerulonephritis.

Design: In this collaborative multi-center retrospective review, thirty-seven patients with a renal biopsy showing glomerulonephritis in the setting of infective endocarditis were identified. All cases were processed by routine light, immunofluorescence and electron microscopy.

Results: The study group included 31 men and 6 women with a mean age of 49 years (range 3 to 84). Predisposing states for endocarditis included a prosthetic valve or ventriculoatrial shunt (28%), intravenous drug use (24%), hepatitis C infection (24%) and valve prolapse or insufficiency (16%). Endocarditis most commonly involved the tricuspid valve (30%) and identified Staphylococcus species on culture. Of the patients tested for ANCA, 63% were negative, 25% were positive, and 13% were equivocal. Serum complement testing was normal in 50% of patients tested. The most common morphologic pattern was diffuse crescentic glomerulonephritis (38%) followed by equal numbers of focal crescentic glomerulonephritis (22%) and diffuse proliferative glomerulonephritis showing endocapillary hypercellularity (22%). Absent or pauci-immune staining for all immunoglobulins was noted in 65% of cases, of which 63% revealed focal or diffuse crescentic glomerulonephritis morphologically. Subepithelial humps were noted by electron microscopy in only 16% of cases.

Conclusions: The majority of patients had renal biopsy findings that were not classic for an infection-associated glomerulonephritis, but rather manifested as pauci-immune crescentic glomerulonephritis. These cases would have been morphologically and clinically suspicious for ANCA-associated glomerulonephritis if the presence of endocarditis was unknown. Positive ANCA serology does not exclude the possibility of endocarditis-associated glomerulonephritis as 38% in this series were either equivocal or positive for ANCA. Also in contrast to the typical infection-associated glomerulonephritis, half of patients tested for serum complement had normal C3 and C4 levels. It is important for the practicing nephrologist and renal pathologist alike to maintain a high index of suspicion for this entity considering the potential adverse outcome if a patient with endocarditis were to be treated with cytotoxic agents in lieu of antibiotics.

1658 Renal Biopsy Findings in 500 Patients with Hepatitis C Virus

CL Boils, PD Walker, CP Larsen. Nephropath, Little Rock, AR.

Background: Hepatitis C virus (HCV) infection has been associated with several glomerular diseases including membranoproliferative-pattern glomerulonephritis (MPGN), membranous glomerulopathy, and fibrillary glomerulopathy. The relative frequency of these diseases in the setting of HCV has not been previously studied in a large case series, to our knowledge. Our aim was to determine the spectrum of renal biopsy findings in patients who are HCV-positive.

Design: By retrospective review, 500 patients with HCV infection who underwent native renal biopsy were identified. All cases were processed by light, immunofluorescence (IF) and electron microscopy. Only cases with adequate diagnostic material were included.

Results: The study group included 343 men and 157 women with a mean age of 53 years (range 14 to 81). Eighteen HCV+ patients had concomitant hepatitis B virus infection and 31 patients were positive for HIV. The most common diagnosis was diffuse and nodular diabetic glomerulosclerosis (DNDGS) (30%), followed by HCV-associated MPGN (20%), arterionephrosclerosis (9.4%), IgA nephropathy (6.2%), membranous nephropathy (5%), acute tubular injury (4.6%), primary focal

segmental glomerulosclerosis (4.2%), and fibrillary glomerulopathy (2.6%). Almost twenty other primary findings were represented in the remaining 18% of cases. In patients with a clinical history of both HCV and DM, only 7% were found to have an HCV-associated GN. The primary indication for biopsy in the 100 patients with HCV-associated MPGN was proteinuria in 59% (mean 6.4 g/day), acute renal failure (38%), and hematuria (26%). Indications for biopsy in patients who proved to have DNDGS without an HCV-associated GN on biopsy were proteinuria (65%, mean 7.2 g/day), chronic kidney disease (20%), acute renal failure (9%) and hematuria (7%). In patients with MPGN, all 21 patients tested showed hypocomplementemia. IF most commonly had positive staining for C3 (92%) and IgM (89%) with mean intensities of 2.1 each (scale 0-3+), followed by IgG in 57% and IgA in 18% (mean intensity 1.6 and 1.8, respectively). Monoclonal light chain restriction was noted in 3 patients with MPGN (2 kappa, 1 lambda).

Conclusions: Renal biopsy revealed a spectrum of findings in patients with hepatitis C virus infection. The fact that DNDGS was the most common finding indicates that nephrologists struggle to differentiate these diseases clinically. Hypocomplementemia is typically present in HCV-associated MPGN, however it is not typically present in the other HCV-associated glomerulonephritides of membranous and fibrillary glomerulopathy.

1659 Renal Hypoplasia: A Review of Thirteen Cases of Two Distinct Types

SM Bonsib, R Fan, R Nair. Louisiana State University Health Sciences Center, Shreveport, LA; Riley Children's Hospital, Indianapolis, IN; University of Iowa Hospitals and Clinics, Iowa City, IA.

Background: Renal hypoplasia (RH) is failure of the kidney to achieve normal size. There are several types that include simple hypoplasia - reduced number of lobes, oligomeganephronia - reduced number of lobes with nephron hypertrophy and Ask-Upmark segmental hypoplasia - reduced lobes with deep cortical grooves representing hypoplastic lobes. Another form not recognized we call cortical hypoplasia; nephrogenesis is normal with marked reduction in nephron generations.

Design: The files of SB were searched for cases of RH not associated with cystic dysplasia or extrarenal malformations. Thirteen cases were identified. The glass slides (13/13), gross photographs (6/13) and medical records (11/13) were reviewed. Nephron generations were counted along medullary rays optimally oriented perpendicular to the capsule.

Results: Thirteen cases of RH included 7 segmental hypoplasia (SegH), 5 cortical hypoplasia (CortH) and 1 with mixed features. All were unilateral. Patients presented with normal creatinine. The hypoplastic cortex in SegH contained a vascular scaffold with thick arteries and numerous veins. Infrequent tubules and no glomeruli occurred in 6/7. One case contained a few normal appearing nephrons. Medullary tissue was absent or consisted of a few tubules in 3/7, or consisted of small islands of immature ducts with ER +/- PR positive mesenchymal collars in 4/7. The CortH cases contained normal appearing lobes with normal labyrinth-medullary ray architecture. Radial nephron counts ranged from 2 to 7 nephron generations per lobe in some or all sections (normal 10-12 generations). The outer medulla appeared normal in 5/5 but the inner medulla lacked thin loops of Henle with increased mesenchymal tissue in 3/3. The mixed case had lobes with CortH while others showed SegH.

Conclusions: (1) Renal hypoplasias are uncommon and rarely reported; this abstract illustrate 2 types (2) Patients had normal renal function since most of the affected kidney is normal and the process is unilateral (4) In SegH the nonhypoplastic lobes are normal. The hypoplastic lobes retain a vascular scaffold of a lobe but lack nephrons. Medullary islands of immature ducts implicate ampullary bud in pathogenesis. (5) We describe 5 cases of CortH, a form not previously described where cortical architecture and nephrons appear normal but with reduced nephron generations indicating premature cessation of nephrogenesis. Either ampullary bud or renal blastema causes may be responsible.

1660 Warfarin Treatment Results in Impaired Renal Function and Morphologic Changes in the 5/6 Nephrectomy Model of Ablative Nephropathy (AN) in Rats, Resembling Warfarin Related Nephropathy (WRN) in Humans

SV Brodsky, KM Ware, A Ozcan, EP Calomeni, G Nadasdy, A Satoskar, T Nadasdy. The Ohio State University, Columbus, OH; Gulhane Military Medical Academy, Ankara, Turkey.

Background: We had previously reported that patients with chronic renal disease on warfarin therapy with INR>3.0 may develop acute kidney injury as the result of glomerular hemorrhage and formation of occlusive tubular red blood cell (RBC) casts. We termed this condition WRN. No animal model is available to study the pathogenesis of WRN.

Design: Herein we report changes in serum creatinine (SC) and morphologic findings in the AN rats treated with increasing warfarin doses at different stages of AN development. Serum creatinine levels, prothrombin time (PT) and hematuria were measured and renal pathology was evaluated.

Results: Warfarin treatment resulted in an increase of PT (surrogate INR) up to 5 folds. The PT increase was accompanied by an increase in SC in AN rats, but not in control rats. The SC increase was more prominent in AN rats treated with warfarin at 19 and 3 weeks (AN 19w, AN 3w) as compared to AN rats treated at 8 weeks (AN 8w) after the ablative surgery.

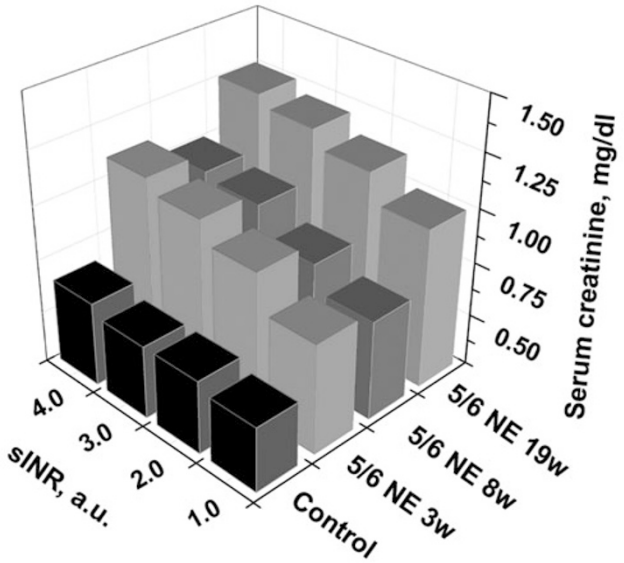

The SC increase was correlated well with PT changes in AN rats, but not in control (R^2=0.567 in AN 19w; R^2=0.310 in AN 8w; R^2=0.570 in AN 3w; R^2=0.054 in control). Warfarin treatment was not associated with blood pressure changes in any of the experimental groups.

Warfarin treated AN, but not control rats had acute tubular injury with RBC and RBC casts in the tubules. Hematuria was increased with PT elevation, more prominently in AN rats. The morphologic changes were more prominent in AN 19w rats as compared to AN 8w and AN 3w rats and worsened with PT elevation. Interestingly, even a small increase in PT (2-3 folds) resulted in tubular RBC and RBC casts formation in AN rats. Treatment with vitamin K prevented SC increase and RBC casts formation associated with warfarin treatment.

Conclusions: 1. Warfarin treatment results in increased SC and morphologic changes resembling human WRN in AN rats; therefore, the 5/6 nephrectomy model of AN is an appropriate animal model to study WRN. 2. Warfarin effects are more prominent with the progression of chronic kidney disease. 3. Vitamin K treatment prevents functional and morphologic changes of WRN.

1661 Banff Initiative for Quality Assurance in Transplantation (BIFQUIT): Inter-Observer and Inter-Laboratory Reproducibility for C4d Immunohistochemistry in Renal Allografts

S Chan, J Climenhaga, P Randhawa, H Regele, Y Kushner, R Colvin, M Mengel. University of Alberta, Edmonton, Canada; University of Pittsburgh, Pittsburgh; University of Vienna, Vienna, Austria; MGH, Harvard Medical School, Boston.

Background: Detection of C4d is crucial for diagnosing antibody mediated rejection in kidney, pancreas, and heart allografts, yet formal reproducibility studies are limited.

Design: We conducted an international multi-center trial to assess the inter-observer and inter-laboratory reproducibility for C4d immunohistochemistry on paraffin-sections. A tissue microarray (TMA) was constructed comprising 44 kidney allograft specimens representing the whole analytical spectrum from negative over mild/focal to strong/diffuse C4d positivity, in cases with acute or chronic antibody mediated rejection. Using TMAs allowed us to distribute essentially identical trial material to 78 participants at 60 institutions. Participating laboratories stained the TMA slides using local protocols. Participants evaluated their slides following the Banff C4d grading schema and entered their scores online. Stained slides were returned for centralized panel scoring. Weighted kappa statistics were used to determine the inter-observer and inter-laboratory reproducibility.

Results: Inter-observer reproducibility for comparing local participant scoring to the corresponding panel scores was fair (kappa 0.39), while inter-laboratory reproducibility based on the panel scores was moderate (kappa 0.49). Inter-observer reproducibility was primarily limited due to cases with focal staining (i.e. C4d 1-2), and could be significantly improved by omitting the Banff C4d grading schema and only considering +/- calls (kappa 0.60). Scoring only C4d+/- the inter-laboratory reproducibility improved considerably (kappa 0.78).

Conclusions: These results indicated that C4d staining on paraffin section is reproducible between laboratories. The Banff grading schema has lower reproducibility between observers, mainly due to cases with mild/focal staining patterns.

1662 C4d Deposition without Recruitment of Inflammatory Cells Is Insufficient To Trigger Microcirculation Injury in Mouse Kidney Allografts

A Chow, P Blanco, L-F Zhu, B Sis. University of Alberta, Edmonton, AB, Canada.

Background: C4d staining is a diagnostic marker for antibody-mediated rejection in human allografts, but has limitations i.e. not highly sensitive or specific (such as in ABO incompatible allografts).

We hypothesized that C4d deposition in capillaries without recruitment of intracapillary inflammatory cells is not sufficient to trigger allograft injury.

Design: We developed an MHC class I mismatched allograft model in the mouse by transplanting CBA (H-2^k) kidneys into B6.RAG1KO (H-2^b) recipients who lack mature B and T cells. To induce the effects of antibody-mediated rejection, three different doses

of anti-mouse H-2K^k monoclonal antibodies were injected: a single injection of 100ug on day 6 post-transplant and harvesting of kidneys 24 hours later (n=3), three injections of 300ug on days 3,5,7 and harvesting 45 minutes after the last injection (n=8), or a single injection of 750ug on day 6 and harvesting 24 hours later (n=3). C4d deposition was visualized by immunohistochemistry. We also examined soluble serum complement component C5a levels by ELISA, and related C4d staining to histopathology, serum C5a levels, and intragraft transcriptome changes, measured by Affymetrix microarrays.
Results: Normal kidneys, CBA or RAG1KO isografts, and RAG1KO allografts without alloantibody treatment were negative for C4d staining. However, all RAG1KO allografts treated with alloantibody showed diffuse C4d staining in glomerular and peritubular capillaries. By histopathology, RAG1KO allografts with alloantibody treatment were negative for increased microcirculation inflammation, thrombi, congestion or other histological features of rejection, thus did not significantly differ from isografts or untreated RAG1KO allografts. Serum C5a levels did not increase in mice with RAG1KO allografts after 100ug and 300ug alloantibody injections ($p>0.05$) and mildy increased following injection of 750ug of alloantibody, but the difference did not reach a statistical significance when compared to serum from untreated RAG1KO allograft recipients. By microarrays, expression of Ifng inducible transcripts, endothelial cell-, and macrophage-associated transcripts did not differ between RAG1KO allografts with alloantibody injection and untreated RAG1KO allografts ($p>0.05$).
Conclusions: We showed that alloantibody-induced capillary C4d deposition is not associated with microcirculation inflammation and intragraft gene expression changes when there is incomplete activation of the complement cascade. Thus C4d protein is an inert molecule and incapable of triggering allograft injury.

1663 2,8 Dihydroxyadeninuria — A Renal Biopsy Case Series

LN Cossey, E Chukwuma, S Nasr, CP Larsen. University of Arkansas for Medical Sciences, Little Rock, AR; Nephrology Associates of Dayton, Dayton, OH; Mayo Clinic, Rochester, MN; Nephropath, Little Rock, AR.
Background: 2,8 dihydroxyadeninuria (DHA) is a rare autosomal recessive disorder caused by a deficiency of adenine phosphoribosyltransferase (APRT) which is frequently misdiagnosed on renal biopsy. It can be treated pharmacologically but causes irreversible renal injury and progression to ESRD if left untreated. This study reports three patients with DHA crystalline nephropathy diagnosed via percutaneous renal biopsy.
Design: In this retrospective review, three cases of DHA crystalline nephropathy were identified. Pathologic description and pertinent clinical data is provided.
Results: Two patients were female, one male; two African American and one Caucasian. Past medical history included hypertension in 2/3 and obesity in 1/3. One patient had a maternal history of CKD. Patients had no history of nephrolithiasis or obstruction. Creatinine levels at presentation ranged from 2.01-10.3 (mean of 5.2). Proteinuria was identified in two patients (550 mg/d and 2 gm/d). Renal biopsies showed a range of 5-42 glomeruli with 7-22% globally sclerotic. Needle-shaped, birefringent brownish yellow crystals were identified in all cases within tubular lumina, tubular epithelial cell cytoplasm, and interstitium, and were positive on silver stain in all cases. Tubular atrophy and interstitial fibrosis was severe in all cases. There was a focal multinucleated giant cell reaction to the crystals in all cases. APRT RBC activity was mildly decreased in one patient, markedly decreased in another, and is unknown in one patient. Two patients have progressed to ESRD, one of whom received a kidney transplant with disease recurrence 4 months post-transplant. The third patient has been lost to follow-up.
Conclusions: DHA is a rare cause of renal disease that can lead to irreversible renal failure. Clinically, there are no distinguishing characteristics of DHA and awareness of this disease among clinicians is low. Morphologically, DHA crystals can be confused with oxalate crystals but can be differentiated by special staining methods. It is important that pathologists be aware of DHA in the differential diagnosis of crystalline nephropathy as it has a poor prognosis and frequently recurs in transplants.

1664 Renal Biopsy in the Very Elderly: Analysis of 833 Native Renal Biopsies

S Dhingra, PD Walker, R Zhang, C Larsen. UT-Health, Medical School, Houston, TX; Nephropath, Little Rock, AR.
Background: Increase in longevity due to better quality of medical care has led to an increase in the demographic subset of the very elderly population (age ≥ 80 years). This has a great impact on health care expenditures. With respect to renal disease, initiation of dialysis in the elderly population leads to a sharp decline in functional status within the first year. Though there are some studies reporting the clinical presentation and cause of renal disease in this subgroup, numbers of patients have been limited. Our study delineates the clinicopathologic correlation and significance of renal biopsies in the largest cohort of very elderly patients reported to date.
Design: Our databank was searched for all native renal biopsies obtained during a 10-year period from 2001 to 2010 in patients aged 80 years or older. The biopsies were received from multiple medical centers across the United States and showed a fair representation of all nephrology practice settings such as small community practice groups to tertiary care referral centers. A total of 833 cases were included. Cases with lack of clinical information or limited biopsy tissue were excluded from the study.
Results: The mean age was 83 years (range 80 to >100) and the male to female ratio was 1:1. The most common indications for renal biopsy were acute kidney injury (AKI) (65%), chronic progressive injury (16%) and nephrotic syndrome (10%). The most common findings in cases biopsied for AKI were pauci-immune glomerulonephritis (22%), acute tubular necrosis (14%) and acute interstitial nephritis (12%). Among cases with AKI, 34% needed immediate therapeutic intervention and 20% required potential modification of treatment, based on biopsy results. Overall arterionephrosclerosis was the most frequent histological diagnosis (17%) followed by pauci-immune glomerulonephritis (15%) and diabetic nephropathy (11%).
Conclusions: Renal biopsy is a valuable diagnostic tool to guide treatment in the very elderly patients, especially in a setting of rising creatinine, in order to prevent progression to end stage kidney disease and dialysis dependence.

1665 The Significance of Tubuloreticular Inclusions (TRIs) in Allograft Kidney Biopsies

CL Ellis, G Gupta, LC Racusen, LJ Arend. The Johns Hopkins Hospital and School of Medicine, Baltimore, MD.
Background: Tubuloreticular inclusions (TRIs) consist of anastomosing tubular structures found within the endothelial cells of glomerular and peritubular capillaries. Historically, they have been referred to as *interferon footprints*, as they are inducible in normal lymphocytes upon exposure to interferon alpha in vitro. Although their precise function or cause remains unknown, it has been reported that they can be seen in native kidneys of patients with lupus nephritis, human immunodeficiency virus infection, and in patients treated with interferon. A previous report showed that in transplanted kidneys, the presence of TRIs was second only to lupus nephritis in terms of total amount, and suggested that their presence in transplants may be associated with procedural ischemia, and not a viral etiology. Our study strives to further determine the significance of TRIs in transplant biopsies.
Design: A search of our computer database revealed renal allograft biopsies in which TRIs were clearly identified as present (n=28) between the period of Jan '08 - Oct' 11. A control group in which TRIs were not described was identified (n=48). A descriptive analysis of patient and biopsy characteristics for the TRI group was performed. The TRI group was compared with the control group for prevalence of viral infections including parvovirus, hepatitis C, hepatitis B and adenovirus, and other clinical and pathologic characteristics.
Results: Only 2 patients in the TRI group had 'classic' pre-transplant associations with TRIs (one each for HIV and lupus). A sizeable proportion (11/28; 40%) of biopsies was obtained from 'high-risk' transplant recipients (ABO incompatible and/or positive-crossmatch). 11/28 (39%) biopsies had some form of allograft rejection based upon Banff criteria. In comparison with the control group (1/48; 2%), the TRI group had a significantly higher prevalence of hepatitis C infection (6/28; 21%), only one of which had been treated with interferon. This latter finding was statistically significant ($p=0.008$).
Conclusions: Based upon our preliminary findings, it appears that the presence of TRIs in renal allograft biopsies is not explained adequately by traditionally reported associations (HIV, lupus or interferon therapy). A diagnosis of hepatitis C should be sought in renal allograft biopsies with demonstrable TRIs. Further analyses are needed to find other putative etiologies for the presence of TRIs, including the observed intriguing preponderance in 'high-risk' renal allografts.

1666 Production of Control Slides for BK Virus Immunostaining/In-Situ Hybridization Using Voided Urine; a Practical Solution for the Renal Pathologist

Y Elshenawy, J Ferris, J Preiszner, PS Randhawa, GA Youngberg. East Tennessee State University, Johnson City, TN; University of Pittsburgh, Pittsburgh, PA.
Background: Maintaining BK virus control material is a common and frustrating problem. BK virus can cause severe tubulointerstitial nephritis leading to graft loss. Detection and confirmation of BK virus in kidney biopsies using immunohistochemical stains (IHC) or in-situ hybridization (ISH) is essential for optimal patient care. The scarcity of BK virus control material is in part attributable to the limited amount of tissue in a renal needle biopsy and to the limited availability of commercial controls.
Design: We implemented a new method to generate positive controls using a voided urine specimen from a patient with BK viremia, previously diagnosed by serum PCR testing. A single voided random urine sample was centrifuged down to pellets, washed with phosphate buffered saline (PBS), combined and re-suspended in PBS to create 5 ml. of a concentrated cell suspension. The pellet was mixed 1:1 with HistoGel, fixed in formalin and finally processed into paraffin-embedded cell blocks. Freshly cut slides were stained with a mouse anti-BK virus large T antigen monoclonal antibody. In addition, five randomly selected cell blocks were submitted for ISH, using a standard technique.
Results: The cellularity of the single voided random urine sample provided us with a generous amount of centrifuged cellular material (50 blocks). Approximately ten positive cells were present per section. The positive cells depicted a brown nuclear stain visible on light microscopy.

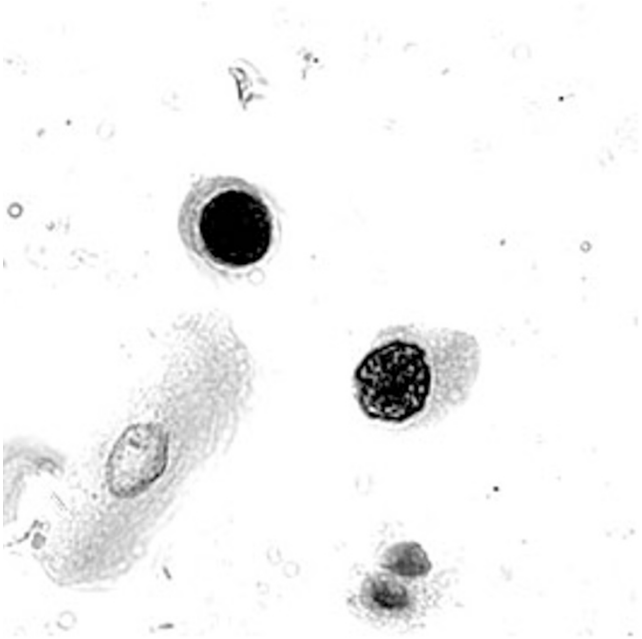

The same results were obtained using the ISH procedure.

Conclusions: The urine-derived cell block method has proven to be helpful in our laboratory for the production of control tissue sections for BK virus IHC. It has been in successful use since 2009. While tissue from renal biopsies represents a more conventional resource for control sections, any positive biopsy used as a control is soon cut through, so a reliable source of control material cannot be maintained. Retrieving cytologic material from urine can be a readily accessible, non-invasive source of positively staining cells for IHC and ISH control purposes. This methodology can be easily implemented in most renal pathology practices.

1667 The Banff Fibrosis Trial: A Multicenter Trial of Visual Assessment of Interstitial Fibrosis in Kidney Biopsies and Its Relationship to Function

AB Farris, S Chan, J Climenhaga, C Bellamy, D Seron, R Colvin, M Mengel. Emory University, Atlanta; University of Alberta, Edmonton, Canada; Edinburgh University, Edinburgh, United Kingdom; University of Barcelona, Barcelona, Spain; MGH, Boston.

Background: Interstitial fibrosis (IF) in renal biopsies is a valuable correlate for organ function, provides prognostic information and is a potential end point in clinical trials.

Design: We conducted a multi-centre trial using 15 allograft and 15 native kidney biopsies with a full range of IF. Sections were stained with trichrome, PAS, or IHC for Collagen III, and scans (Aperio) were prepared for scoring. Trichrome and PAS stained slides were assessed by 27 pathologists following two different definitions of IF (figure 1): (A) the % cortex surface occupied with fibrous tissue. (B) the % cortex which has abnormal fibrosis. Reproducibility was assessed using kappa statistics. The results were correlated with collagen III IHC computer based image analysis (reference standard). All five approaches for assessing IF as well as the extent of tubular atrophy and the Banff total cortical inflammation (ti) score, both visually on the PAS stain, were correlated to organ function (GFR).

Results: Using the trichrome stain better correlations with the collagen III IHC were obtained compared to the PAS stain. Approach B, i.e. estimating the % abnormal cortex, was superior to approach A (Table 1). A stronger inverse association between IF and GFR was seen with the trichrome stain, using either A or B methods. Tubular atrophy and the Banff total i-score correlated less well with the collagen III stain and GFR. Independent of the approach and the stain, reproducibility between observers for assessing IF was weak (kappa <0.25 compared to collagen IHC), while the ti score showed fair to moderate reproducibility.

Figure 1

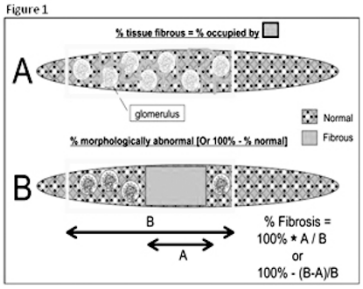

Table 1: Spearman correlations: mean r-values derived from the 27 participant scores are given for the listed associations between the two stains and the two scoring approaches with Collagen IHC and GFR.

	Approach A PAS Stain	Approach A Trichrome Stain	Approach B PAS Stain	Approach B Trichrome Stain	Tubular Atrophy PAS stain	Total I-Score	Collagen III immunohistochemistry
Collagen III immunohistochemistry	0.50	0.61	0.57	0.66	0.57	0.18	
GFR-Cockroft - Gault	-0.36	-0.42	-0.39	-0.43	-0.40	-0.22	-0.44

Conclusions: The trichrome stain is superior to the PAS stain in assessing IF. Pathologists are better capable of assessing the extent of abnormal cortex than the extent of interstitial space occupied by fibrous tissue. Visual assessment of IF in a trichrome stains correlates with organ function as well as computer-based image analysis of collagen III IHC. Significant variability between observers argues that more precise consensus criteria are needed for measuring IF visually.

1668 Pathology of Kidney Injury in Septic Patients

JP Gaut, O Takasu, PE Swanson, RS Hotchkiss. Washington University School of Medicine, St. Louis, MO; University of Washington, Seattle, WA.

Background: Acute kidney injury (AKI), defined clinically as a rapid increase in serum creatinine, complicates 30-60% of patients with sepsis. Such patients require intensive care, but mortality is unacceptably high (70%). The mechanistic basis for renal dysfunction in sepsis is poorly understood. There is currently an urgent need for standardizing diagnostic AKI criteria particularly for new AKI targeting therapies. Renal biopsy is rarely performed for septic AKI and therefore there is little pathologic data from humans. It is the aim of this study to evaluate the renal histopathology of septic AKI.

Design: Rapid postmortem kidney tissue harvest was performed at the bedside (n=26). Control specimens were retrospectively obtained from trauma and oncologic patients who underwent partial or total nephrectomy (n=21). Tissues were examined for apoptosis and necrosis by light microscopy and by immunohistochemical staining for KIM-1, active caspase-3, cytokeratin-18, and cleaved PARP. Acute tubular injury (ATI) and KIM-1 staining were quantified as the percentage of injured tubules per 200 tubular cross-sections.

Results: Light microscopy showed relatively mild alterations in septic kidneys. Tubular dilatation, epithelial flattening, and rare necrosis was seen in the renal cortex of 77% of septic cases, affecting an average of 6±1.2% of cortico-medullary junction (CMJ) tubules, and 1.2±0.4% of cortical tubules. In contrast to the mild light microscopic findings, KIM-1 was more sensitive for detecting ATI, highlighting 22% of the CMJ tubules and 12% of the cortical tubules, on average. Active caspase-3, cytokeratin-18, and cleaved PARP showed only rare staining. Interestingly, the medulla showed more frequent tubular necrosis in septic kidneys, affecting all septic patients, with an average of 22±2.4% of tubules injured. The remaining histologic findings were minimal.

Conclusions: These results support the hypothesis that ATI plays a role in the pathophysiology of septic kidney injury, but the pathologic findings are subtle. The CMJ and medulla are particularly susceptible to injury compared with the cortex. KIM-1 facilitates the diagnosis and may be a useful marker for standardizing the histopathologic criteria for ATI. Apoptosis does not appear to be a major mechanism of cell death in septic AKI. This investigation of lethal septic AKI in humans 1 hour after death provides unique insights into the underlying mechanism of septic renal dysfunction in humans.

1669 Transplant Glomerulopathy and Dual Disease: An Uncommon Occurrence in Renal Allograft Biopsies

S Gottipati, S Wagner, E Vasquez-Martel, J Gaut, H Liapis. Washington University, St Louis, MO; Complejo University Hospital, La Coruna, Spain.

Background: Transplant glomerulopathy (TG) and recurrent glomerular disease are currently leading causes of renal allograft loss. Alloimmunity underscores TG in most cases and is a target for intervention. Whereas, both TG and recurrent glomerular disease are independent risk factors for decreased graft survival, the effect on outcome of concurrent TG and recurrent native glomerular disease has not been investigated.

Design: A retrospective review of the renal biopsy databases at Washington University in St. Louis and the Complejo University Hospital, La Coruna, Spain was performed. Clinical, laboratory data and follow up were collected. The biopsies were evaluated for acute/chronic rejection, IFTA, C4d deposition, cyclosporine toxicity and glomerular pathology. TG was scored on electron microscopy 1-3+ as follows: g1: subendothelial edema; g2: segmental glomerular basement membrane (GBM) duplication or multilamellation; g3: diffuse GBM duplication.

Results: 9 cases (from 1182 allograft biopsies) with dual glomerular disease were identified. TG with concurrent IgA (n=5), TG with DDD (n=1), TG with membranous glomerulonephritis (n=1), TG with collapsing glomerulopathy (n=1) and TG with thrombotic microangiopathy involving the glomeruli (n=1). Mean age was 47 ± 13 years; average 7.5 ± 7.9 years from transplant to biopsy. Mean follow up after diagnosis of TG

was 1.7 ± 1.8 years. Mean proteinuria was 1802 ± 2685 mg/day at biopsy and 2252 ± 3210 mg/day at 1 year after biopsy. One pt. had acute rejection. IFTA 1-2+ was seen in all cases; chronic CNI in 3; acute glomerulitis in 2. Glomerular C4d+ in all cases but 1 IgA. Focal (2+) or diffuse (4+) C4d in PTC was present in 6; 3 IgA were C4d-. TG score was g1 in 3 (all IgA); TG g2 in 3 (2 IgA and 1 TMA) and TG=g3 in the rest. Two patients with concurrent IgA lost their graft 8 days and 38 months respectively. One pt with CNI toxicity, TG g2 and IgA had persistent functional decline and was re-listed for transplantation. 75% (6/9) of patients had slow renal function decline.

Conclusions: Dual disease is rare in allograft renal biopsies; TG with concurrent IgA is the most frequent. The distinct electron microscopic findings of TG are essential for definitive diagnosis of superimposed glomerular diseases. Rapid graft loss is more frequent in advanced TG with other co-existing risk factors, e.g., cyclosporine toxicity, or acute rejection, not just concurrent disease.

1670 Renal Medullary Angiitis

A Hendricks, A Harris, P Walker, C Larsen. Nephropath, Little Rock, AR.

Background: Renal medullary angiitis is a lesion seen in small vessels involving the vasa recta of the renal medulla. It consists of interstitial hemorrhage with associated karyorrhexis and polymorphic inflammatory infiltrate surrounding the peritubular capillaries in the medulla. A PubMed review revealed a total of 15 cases of medullary small vessel vasculitis in three publications, all of which were in the setting of ANCA-associated disease. The scarcity of cases in the literature detailing this lesion is likely due to a lack of medullary tissue in many biopsies, and due to the fact that it is often mistaken for acute interstitial nephritis.

Design: We searched our renal biopsy cases from January 2008 through August 2011 and identified 38 cases of medullary angiitis. All cases were examined by light microscopy, immunofluorescence, and electron microscopy. The clinical history submitted at the time of renal biopsy was reviewed and pertinent information including patient's age, gender, indication for biopsy, serum creatinine, and any positive serologic tests, including ANCA, was collected.

Results: Acute renal failure was the indication for biopsy in 29/38 (76%) cases, while rapidly progressive renal failure was second at 16%. In total, 23 (60.5%) cases of medullary angiitis were determined to be ANCA-associated while 15 (39.5%) were determined to be secondary to other etiologies. The most common non-ANCA etiology of medullary angiitis was IgA nephropathy (18.4%) followed by antibiotic treatment in the setting of infection (15.8%). There was also one patient with cryoglobulinemia and one patient with salicylate toxicity. Twenty-seven showed focal involvement of the medulla and 11 had diffuse involvement. ANCA-associated cases showed diffuse involvement in 7/23 while non-ANCA cases showed diffuse involvement in 4/15. There was no involvement of renal cortex in any of the 38 cases.

Conclusions: To our knowledge, this is the largest study to date detailing the morphological and clinical spectrum of renal medullary angiitis. This is an important lesion to recognize because in the majority of cases its presence suggests systemic vasculitis, which should prompt ANCA serologies. If ANCA serologies are negative and there is no evidence of IgA nephropathy, then a drug-induced etiology should be considered. When interstitial hemorrhage and/or inflammation are present in the medulla on renal biopsy, close inspection should be undertaken to exclude the presence of medullary angiitis. This lesion can be seen outside the setting of ANCA-associated disease, and in our series was also present in IgA nephropathy, drug toxicity, and cryoglobulinemia.

1671 Cryoglobulinemic Nephropathy: Spectrum of Clinical and Immunomorphologic Manifestations

GA Herrera, EA Turbat-Herrera. Nephrocor, Orlando, FL.

Background: Thc clinical and pathologic manifestations of cryoglobulinemic nephropathy (CN) are heterogeneous. This is in part due to the fact that this disease is cyclical resulting in variable concentrations of cryoglobulins in the serum affecting renal patterns of damage. Light and immunomorphologic manifesations in renal biopsies are quite variable and only reported in small series. This is the largest series of CN cases in the literature.

Design: 3300 renal biopsies from 2 institutions over a period of 5 years were reviewed to identify cases of CN. Twenty six cases from 25 patients were found. Light, immunofluorescence, and ultrastructural findings were critically analyzed to obtain a comprehensive view of the spectrum of clinical and immunomorphologic renal manifestations.

Results: 0.8% of all renal biopsies were diagnosed with CN. There were 17 male and 8 female patients. Their age ranged from 27 to 81 and the mean age was 54 years. Clinical manifestations were quite varied with acute renal failure (35% of all cases), proteinuria (some associated with nephrotic syndrome), and arthritis being the most common. Associated renal diseases were present in most cases with hepatitis C being the most common (in 46% of the patients), followed by systemic lupus erythematosus, and monoclonal gammopathy of unknown significance (MGUS).

The most common light microscopic appearance was that of a membranoproliferative glomerulonphritis (50% of the cases0, followed by proliferative/exudative variants (12%). Capillary thrombi were seen in 65% of the cases, representing the most constant finding by light microscopy.

Immunofluorescence patterns, though all granular, were also variable. "Full" house fluorescence was present in 40% of the cases. C3 staining was the most constant finding (in more than 75% of the cases).

Electron microscopy showed variable ultrastructural appearances of cryoglobulins including annular, curved, and paired short microtubular structures. No fingerprints, fibrillary, or crystalloid forms were seen.

Conclusions: The immunomorphologic patterns associated with CN are quite heterogeneous. The most common light microscopic finding was that of capillary thrombi associated with variable proliferative/exudative changes. Differential diagnosis included a variety of proliferative/exudative glomerulonephritis. A final, unequivocal diagnosis was only possible ultrastructurally by finding diagnostic substructures in the electron dense deposits, best detected in the capillary thrombi when present and, if absent, in subendothelial deposits.

1672 A Human Glomerular Transcriptional Profile of Endocapillary Proliferation Based on the Oxford Classification of IgA Nephropathy

JB Hodgin, C Berthier, R John, E Grone, S Porubsky, H-J Grone, M Kretzler, H Reich. University of Michigan, Ann Arbor, MI; German Cancer Research Centre, Heidelberg, Germany; University of Toronto, Toronto, Canada.

Background: Our ability to identify patients at risk of progression in IgA nephropathy is inadequate and our understanding of the heterogeneous mechanisms responsible for loss of kidney function in this disease is limited. Recently, the Oxford classification of IgA nephropathy identified the presence of endocapillary proliferation as an independent predictor of renal-function decline. Our goal is to elucidate molecular mechanisms contributing to the development of endocapillary proliferation and subsequent loss of renal function.

Design: We analyzed human glomerular mRNA expression profiles obtained from microdissected kidney biopsies from an international cohort of 22 patients with IgA nephropathy. Biopsies were scored independently using the Oxford classification by three pathologists and a consensus score was generated. A list of differentially regulated genes ($q<0.05$) was generated for further analysis by comparing biopsies with endocapillary proliferation (E1; n=7) versus those without (E0; n=15).

Results: The E1 vs E0 comparison yielded 186 differentially expressed genes highly enriched for a macrophage expression signature. Gene ontology analysis revealed overrepresentation of biological processes related to proliferation and the cell cycle. Overrepresented canonical pathways included the E2F transcription factor network, and the FOXM1 transcription factor network, both of which play key roles in cell cycle progression. Furthermore, upregulation of multiple genes, including FOXM1, were significantly correlated with GFR. Foxm1 may be a therapeutic target for inhibition because it appears to be required for macrophage recruitment. Additional possible targets for therapeutic intervention in our dataset include the chemokine receptor CCR1 and the integrin ITGAM. Finally, we detect injury induced gene expression likely in mesangial cells (C5aR1, TNFAIP8) and endothelial cells (OSR1).

Conclusions: Defining the molecular pathways activated in the IgAN subgroup with endocapillary proliferation gives insight into mechanism of this progressive lesion. Macrophages have been described as key players in IgAN, but no study has yet analyzed an intraglomerular macrophage transcriptomic signature. This approach will allow further elucidation of important pathogenic pathways in IgAN progression, and may reveal new therapeutic targets for further analysis.

1673 The Clinico-Pathologic Spectrum of Rhabdomyolysis and KIM-1 Immunohistochemistry in Patients with Acute Kidney Injury

HE Karnes, JP Gaut, O Takasu, H Liapis. Washington University in St. Louis, St. Louis, MO.

Background: Rhabdomyolysis is associated with acute kidney injury (AKI) and can be lethal. Small decrements in renal function are thought to contribute to increased mortality. Therefore, early AKI detection is crucial. Pathologic changes on renal biopsy may be subtle, underestimating the degree of acute tubular injury (ATI). Previous studies have demonstrated upregulation of kidney injury molecule-1 (KIM-1) within the proximal tubule brush border in patients with AKI. We aimed to investigate whether KIM-1 immunohistochemistry in renal biopsies of patients with rhabdomyolysis may improve assessment of AKI.

Design: A retrospective review of patients at our institution with clinical diagnoses of rhabdomyolysis and renal biopsies performed between 1/1/1989 and 9/1/2011 was conducted. Formalin-fixed paraffin-embedded tissue sections stained with H&E, myoglobin, and KIM-1 were evaluated. The extent of immunohistochemical staining was semiquantitated as follows: 1+ = 1-25% of tissue section staining; 2+ = 25-50%, and 3+ = >50%. Myoglobin and KIM-1 scores were calculated. Clinical follow up at the time of release from the hospital or at autopsy was recorded.

Results: Ten cases were identified with clinical evidence of rhabdomyolysis secondary to HIV (n=1), cocaine use (n=2), membranous glomerulonephritis (n=2), polymyositis (n=1), acute renal failure (n=2), chemotherapy (n=1), heat exhaustion (n=1), and pulmonary hemorrhage (n=1). Apparent ATI was identified in 2/10 (20%) cases. Myoglobin casts were present in 4/10 (40%) biopsies. Eight cases had tissue remaining for KIM-1 immunostaining. KIM-1 (3+) was present in all 4 cases with myoglobin casts, as well as 3 additional cases without casts for a total of 7/8 (88%). The case without KIM-1 staining showed no ATI by light microscopy. Of the patients with 3+ KIM-1 staining, 2 ended up on dialysis, 1 showed progressive decline in renal function and is awaiting transplantation, and 1 died.

Conclusions: Of the patients with clinical rhabdomyolysis, ATI was only identified in 20% of cases. Strikingly, KIM-1 revealed extensive AKI, even when only subtle changes were observed by light microscopy. Diffuse KIM-1 immunoreactivity was associated with a worse clinical outcome. We suggest that KIM-1 is a useful tool for AKI diagnosis and in determining severity in patients with rhabdomyolysis.

1674 Apolipoprotein A1 Genotypes Correlate with FSGS in HIV-Positive African-American Patients

M Kuperman, K Skorecki, T Shemer, W Wasser, L Racusen, D Fine. Johns Hopkins Hospital, Baltimore, MD; Rambam Health Care Campus, Haifa, Israel.

Background: *Apolipoprotein A1 (ApoL1*) polymorphisms have been closely associated with chronic kidney disease in the African-American population. It is estimated that more than 30% of African-Americans carry the two alleles G1 (342G:384M) and G2 (rs71785313). In the HIV-positive population, greater than 50% of individuals who are homozygous or heterozygous for *ApoL1* G1/G2 polymorphisms will develop focal segmental glomerulosclerosis (FSGS) or HIV-associated nephropathy (HIVAN). Our study is designed to further clarify if a particular combination of alleles in HIV affected African-American patients is predictive for developing FSGS in non HIVAN patients.

Design: Kidney biopsies from HIV-positive African-American patients were collected from the archives of Johns Hopkins Hospital from January 1996-January 2009. Biopsies where DNA could not be extracted and biopsies with the diagnosis of HIVAN were excluded. Direct genotyping of 342G:384M and rs4821480 were performed by extracting genomic DNA from the paraffin-embedded tissue (QuickExtract FFPE DNA Extraction Kit) and then concentrating the DNA using DNA Clean & Concentrator 5. IRB approval was received from Johns Hopkins Medical School (04-12-23-02).

Results: 140 kidney biopsies from HIV-positive patients were collected and 97 met inclusion criteria. 29% of the patients were either homozygous or compound heterozygous for G1/G2. Out of the 28 homozygotes or compound heterozygotes, 86% had FSGS, 10% had hypertension, and 4% had immune-mediated glomerulonephritis. 71% of the patients had only one G1/G2 allele haplotype or no G1/G2 alleles. Out of the 69 individuals in this population, 20% had FSGS, 3% had hypertensive nephropathy, 16% had diabetic nephropathy, 41% had immune-complex GN, and 32% had other diagnosis (minimal change, pyelonephritis, etc.)

Correlation of Apolipoprotein A1 Genotype and Histological Diagnosis

	G1/G1	G2/G2	G1/G2	0/G2	G1/0		0/0
FSGS (Classic)	6	3	15	3	8		3
HTN Nephrosclerosis	1	0	2	0	0		2
Diabetic Nephropathy	0	0	0	0	4		7
Immune Complex GN	0	0	1	7	11		10
A. Lupus-Like				(2)	(4)	(2)	
B. B. Post-Infectious					(6)	(1)	
C. IgA			(1)	(2)	(1)	(3)	
D. MPGN				(1)		(1)	
E. Misc.				(2)		(3)	
Other				7	4	3	

Conclusions: Patients who are homozygous or heterozygous for *ApoL1* G1/G2 develop FSGS in a disproportionately large number (86%). By contrast, patients who have non-G1/G2 alleles of *ApoL1* are less likely to develop FSGS. We plan to further investigate these findings to possibly form a predictive test for FSGS and HIVAN in African-American HIV affected patients.

1675 Obstetric Complications, Snake Bites and Indigenous Medicines Account for Nearly Half the Cases of Biopsied Acute Kidney Injury in Southern India

AA Kurien, M Mathew, G Abraham. Madras Medical Mission, Chennai, Tamil Nadu, India.

Background: Acute kidney injury (AKI) in the tropics is strikingly different from that in the western world in terms of etiology and presentation. With increasing opportunities for travel and work to various parts of the world, a working knowledge of these tropical diseases is imperative for the western world.

Design: All native kidney biopsies reported in the past 5 months (May 2011 to September 2011) in the renal pathology division of a tertiary care referral centre in southern India were analysed. We receive biopsies from rural as well as urban regions. Patients who had a clinical presentation of acute kidney injury were included in this study. Clinical details as specified by the referring clinician, along with the histopathological (light and immunofluorescence microscopy in all cases and immunohistochemistry for myoglobin, when applicable) findings were evaluated.

Results: Of the 470 native kidney biopsies, acute kidney injury was the indication for biopsy in 50 (10.6%) patients. This included 27 men and 23 women. The mean age was 35.7 years (ranging 13 years to 70 years).

Results

Clinical history	Number	Histopathological findings
Obstetric complications	9	Cortical necrosis(5) TMA(2) ATN(2)
Snake bite	7	ATN (3) AIN(2) Cortical necrosis(1) Rhabdomyolysis(1)
Traditional/indigenous medicines	7	AIN(6) ATN(1)
Bacterial infections/sepsis	6	ATN(3) PIGN(2) AIN (1)
AKI of unknown etiology	5	PIGN (3) ATN(1) AIN (1)
Pyrexia of unknown origin	4	Rhabdomyolysis(1) PIGN(1) AIN(1) Acute pyelonephritis with microabscess(1)
Falciparum malaria	3	ATN(1) AIN (1) TMA (1)
Leptospirosis	3	Rhabdomyolysis (2) ATN(1)
Diarrhoea/vomiting	3	ATN(3)
Mismatched blood transfusion	1	ATN(1)
Poisoning	1	ATN(1)
Wasp sting	1	AIN(1)

ATN- Acute tubular necrosis, AIN- Acute interstitial nephritis, TMA- Thrombotic microangiopathy, PIGN- Post infectious glomerulonephritis

In the 470 native kidney biopsies evaluated, there were 32 cases of post infectious glomerulonephritis (PIGN). Among these, 6 adult patients presented as acute kidney injury and were included in this evaluation.

Conclusions: This study emphasises some causes of AKI which are unusual to the Western world.

1) Obstetric complications, snake bites and indigenous medicines account for nearly half the cases of biopsied AKI in Southern India

2) Unsupervised consumption of traditional /indigenous medicines causes acute interstitial nephritis.

3) PIGN is still an important cause of AKI in adults.

1676 Prospective Monitoring of BK Viremia and Early Protocol Biopsies: Impact on the Evolution of BK Polyomavirus Associated Nephropathy (BKPVAN). A Kidney Transplantation Center Experience

M Latour, E Renoult, M Paquet, C Girardin, G St-Louis, R Levesque, H Cardinal, M-C Fortin, M-J Hebert, W Schurch. Centre Hospitalier de l'Université de Montréal, Montréal, QC, Canada.

Background: BKPVAN is a major cause of renal allograft dysfonction. The timing of the initial diagnosis is critical for therapeutic success and a good outcome.

Design: A pre-emptive strategy based on prospective monitoring of BK viremia during the first year and allograft biopsies, as part of protocol surveillance at 3 and 6 months, were established in our institution since 2008. We retrieved all cases of BKPVAN diagnosed on biopsy with SV40 positivity from 2004 to 2010. Clinical and histopathological findings were analysed between cases diagnosed before and after 2008.

Results: 21 cases were identified. 11 cases before 2008 (A group) and 10 cases after 2008 (B group). Seven cases were diagnosed on protocol biopsy: 1 in A group and 6 in B group. Time between graft and BKPVAN diagnosis decreased significantly (p=0.0004) after 2008 with an average of 515 days (169-1005) in A group and 143 days (75-243) in B group. eGFR at the time of diagnosis was not statistically different between A and B group (34.9±18.7 and 39.84±12.9). However, one year after BKPVAN diagnosis, eGFR was significantly (p=0.02) better in B group (39.82±14.48) compared to A group (24±12.5). 8 cases in A group have lost more than 20% of renal function compared to only 2 in B group (p=0.03). The majority (7 out of 10) of cases diagnosed after 2008 were staged as early infection (class A).

Conclusions: The introduction of a pre-emptive strategy based on prospective monitoring of BK viremia during the first year and allograft biopsies, as part of protocol surveillance, have modified the evolution of BKPVAN. BKPVAN are now diagnosed earlier with a better outcome. However, some cases still have an aggresive behavior.

1677 Effect of Sirolimus and Cyclosporine on Regulatory T Cells in Renal Transplant Allograft

W Li, PL Zhang. William Beaumont Hospital, Roy Oak, MI.

Background: Regulatory T cells (Tregs) have been shown to prevent rejection and lead to improved long-term outcomes. Sirolimus and cyclosporine are wildly used to treat graft rejection, and are known to modulate lymphocyte cellular division and proliferation. The role and effect of these drugs on Tregs in allograft kidney are unclear.

Design: Formalin-fixed paraffin-embedded tissue sections of 66 renal allograft biopsies were immunostained for three markers of Tregs (Foxp3, CD4, and CD8). The number of positive cells in interstitium and tubules was quantified and the data were expressed as the number of cells/mm^2. The results were compared with biopsies from 16 cases treated with Sirolimus only (Siro), 32 with Sirolimus and Cyclosporine (Siro+Cyclo) and 18 with Cyclosporine only(Cyclo). Clinically relevant levels of proteinuria at the time of biopsy were analyzed in all cases.

Results: The numbers of Foxp3+, CD4+ and CD8+ T cells in interstitium and tubules of renal allograft were significantly greater in Siro group than those in Siro+Cyclo group and Cyclo group. (P<.05 and P<.01, respectively). No significant difference of expression of these regulatory T cells was observed between Siro+Cyclo group and Cyclo group [Table 1]. Proteinuria was significantly higher in Siro (2.98 ± 0.51 g/day) and Siro+Cyclo (2.25 ± 0.41 g/day) groups than Cyclo group (0.71 ± 0.12 g/day (p<0.05).

Table1: Numbers of Foxp3+, CD4+ and CD8+ T cells in interstitium and tubules of renal allograft

Treatment Group (cases)	Foxp3+	CD4+	CD8+
Siro only (16)	9.4 ± 2.4	135 ± 42	261 ± 75
Siro+Cyclo (32)	4.6 ± 1.7	87 ± 27	135 ± 54
Cyclo only (18)	3.1 ± 1.2	79 ± 24	129 ± 39

The number of positive cells in interstitium and tubules was quantified and the data were expressed as the number of cells/mm2

Conclusions: Sirolimus appears to increase the number of Tregs whereas cyclosporine decreases the number of Tregs in allograft kidney, suggesting that immunosuppressive drugs have differential effects on Tregs. Examination of expression of Tregs may have the potential to inform immunosuppressive regimen manipulation to improve outcomes of allograft. Our results also confirm previous reports of a significant increase of proteinuria in kidney transplant recipients treated with Sirolimus.

1678 The Banff Schema for Allograft Pathology: Revisiting Scoring Paradigms for Inflammation and Tubulitis

L Liu, P Randhawa. University of Pittsburgh, Pittsburgh.

Background: Diagnostic categories in the Banff Schema are based on evaluation of non-scarred areas for inflammation (Banff-i) and tubulitis(Banff-t). We investigated how diagnostic algorithms might be affected by (a) presence of severe inflammation which can mask tubular disruption and lead to under-grading of tubulitis (Banff-t), and (b) replacement of Banff-i by a total inflammatory score (ti) encompassing both scarred and non-scarred areas.

Design: To study potential under-grading of tubulitis, ~2000 biopsies were retrieved for review and 14 cases scored as i3t1v0 were rescored for Banff-i, ti, Banff-t, and t-total (defined as peak tubulitis in scarred or unscarred cortex). Tubulitis was not scored in areas with greater than mild atrophy recognized by (a) tubular basement membrane thickening or (b) >50% decrease in tubule diameter.

Results: 12 of 14 retrieved cases showed tubular disruption, which led to upgrading of tubulitis from t1 to t3. The remaining 2 cases showed tubulitis only in tubules with significant atrophy and were not further considered.

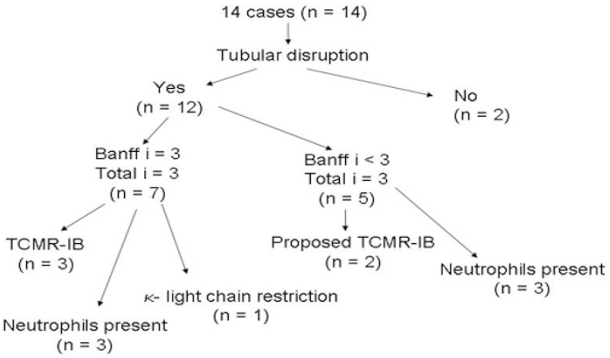

Biopsy review using conventional Banff criteria altered the diagnosis from 'Borderline change' to T-cell mediated rejection (TCMR)-Type 1B in 3 cases, one of which was C4d positive. Two (2) cases with ti=3, Banff i<3, and tubular disruption were found. Given recent evidence that ti correlates well with intra-graft molecular disturbances (AJT 2009:9:1859), it is proposed that the latter biopsies also be classified as TCMR-Type 1B. In 6 biopsies (3 in the Banff-i=3 group, 3 in the Banff-i<3,ti=3 group), interpretation of TCMR–like changes was confounded by concurrent findings suspicious for infection (neutrophilic tubulitis, intra-tubular neutrophil clusters), and another biopsy (Banff-i=3 group) showed κ-light chain restricted plasma cells.

Conclusions: Biopsies where an initial evaluation suggests a score of i3t1 should be evaluated for antibody mediated rejection and urinary tract infection. The presence of tubular disruption should be sought as this may lead to an upgrading of TCMR. Some biopsies show tubular disruption with a ti=3 but Banff-i score of 1 or 2: given recent evidence that ti is superior to Banff-i in predicting graft dysfunction, we propose that these biopsies also be considered TCMR-type 1B, pending validation by future studies.

1679 Reproducibility of the Columbia Classification of Lesions of Focal Segmental Glomerulosclerosis

SM Meehan, A Chang, I Gibson, L Kim, N Kambham, Z Laszik. University of Chicago, Chicago, IL; University of Manitoba, Winnipeg, Canada; Stanford University, Stanford, CA; Univeristy of California San Francisco, San Francisco, CA.

Background: The Columbia working classification of focal segmental glomerulosclerosis (FSGS) identifies 5 types of lesions, designated collapsing (COLL), cellular (CELL), glomerular tip lesion (GTL), perihilar (PH) and not otherwise specified (NOS) types. This study examined interobserver reproducibility of criteria for classification of glomerular morphologic lesions of FSGS.

Design: Sixty-one 400x digital images of FSGS lesions, stained by PAS or Jones methenamine silver methods, were examined by six renal pathologists. Each image was classified independently by each observer using Columbia criteria. Criteria used for classification of lesions were tabulated by each observer. Lesions were considered diagnostic when a majority of opinion favored a single diagnosis.

Results: The percentage of overall agreement was 75.2% with a kappa value of 0.69, indicative of substantial reproducibility. Complete agreement (6 of 6 observers) occurred in 31 of 61 (50.8%) of cases. Consensus by 4 or more observers was attained in 86.9% of instances. Diagnostic disagreement by category is shown in the Table.

Discrepant Diagnoses

	Other Diagnoses Rendered				
Majority Diagnosis (# cases)	COLL	CELL	GTL	NOS	PH
COLL (n=5)	-	4	1	3	0
CELL (n=7)	3	-	2	5	0
GTL (n=2)	0	2	-	0	0
NOS (n=12)	0	7	4	-	2
PH (n=0)	0	0	0	0	-

Interpretation of capillary retraction and endocapillary hypercellularity accounted for disagreement in COLL v CELL and COLL v NOS. Different interpretation of endocapillary hypercellularity accounted for disagreement in CELL v NOS. Disagreement about location of lesions explained discrepancies in interpretation of GTL and PH lesions.

Conclusions: Columbia criteria for morphologic lesions of FSGS are substantially reproducible between experienced observers and provide a robust method for assessment of the varied morphologic manifestations of this lesion.

1680 Integrin alpha-v-beta 6 Protein Expression in Human Renal Allograft Biopsies: A Marker of Nephron Distress

M Mengel, S Chan, K Famulski, J Chang, J Reeve, S Violette, P Weinreb, P Halloran. University of Alberta, Edmonton, Canada; Stromedix Inc., Boston; Biogen Idec Inc., Boston.

Background: Integrin alpha-v-beta 6 (avb6) is expressed on stressed epithelium, where it activates latent TGF-β1 in the adjacent interstitium.

Design: We stained 123 human renal allograft biopsies for cause (BFC) and 67 six-week protocol biopsies to examine the relationship between avb6 staining and expression of avb6- and TGF-β regulated transcripts, histological lesions, allograft function and outcome.

Results: Staining for avb6 was confined to epithelial cells, and presented two patterns: basolateral and cytoplasmic. The avb6 staining correlated with beta-6-integrin mRNA expression (r=0.41, p<0.001), and with transcripts regulated by avb6 (r=0.29, p=0.004) and TGF-β1 (r=0.28, p<0.001). Staining by avb6 correlated positively with inflammation, fibrosis and atrophy, and showed cytoplasmic accumulation in atrophic tubules, but did not correlate with histological lesions of acute kidney injury. Staining was observed across many injury and disease entities, in early and late biopsies. Cytoplasmic avb6 staining was associated with prior DGF (p=0.029) in protocol biopsies. In early BFC (<1 year post transplantation) with acute kidney injury increased avb6 staining was the only biopsy feature associated with reduced eGFR (table 1). In late BFC with progressive diseases avb6 staining was associated with inferior allograft survival (p=0.006).

Table 1: Results from ROC curve analysis for predicting allograft function at time of biopsy in the various sub-sets of clinically indicated biopsies for cause (BFC). The Area Under the Curve (AUC) from each analysis is given for histology lesions and avb6 staining results.

*normal histology includes a group of BFC showing only features of acute kidney injury (AKI), i.e. biopsies from the early post transplant period (<42 days post transplantation) showing no histological evidence of rejection or any other specific diseases. Also included are BFC showing no major abnormalities, i.e. BFC taken >42 days but <1 year post transplantation, fulfilling no Banff diagnostic criteria and showing only minor histopathological abnormalities (Banff ci-score ≤1).

Variable	All BFC AUC (n=123)	Early BFC (<1 year post transplantation) AUC (n=45)	Late BFC (>1 year post transplantation) AUC (n=78)	Early BFC with normal* histology AUC (n=18)
any αvβ6 staining	**0.60**	**0.63**	0.59	**0.86**
basolateral αvβ6 staining	**0.61**	0.60	**0.64**	**0.86**
cytoplasmic αvβ6 staining	0.54	0.62	0.51	**0.71**
Banff C4d score	0.51	0.50	0.51	0.50
Banff i-score	0.59	**0.67**	0.45	0.34
Banff total i-score	**0.62**	0.61	**0.63**	0.61
Banff t-score	0.47	**0.62**	0.54	0.50
Banff v-score	0.47	0.43	0.50	0.50
Banff g-score	0.49	0.52	0.47	0.55
Banff cg-score	0.50	0.43	0.54	0.50
Banff mm-score	0.48	0.59	0.51	0.70
Banff ci-score	0.55	0.53	0.60	0.45
Banff ct-score	0.56	0.52	**0.63**	0.48
Banff cv-score	0.57	0.57	0.59	0.65
Banff ptc-score	0.46	0.47	0.45	0.50
Histological signs of acute epithelial injury	0.50	0.61	0.56	0.70

Conclusions: Thus avb6 staining is an indicator of epithelial distress and provides mechanistic insights by its association with avb6- and TGF-β regulated transcripts. Increased avb6 protein expression in tubular epithelial cells correlates with dysfunction, and future progression to allograft failure.

1681 Best Practice for C4d and BK Staining in Paraffin Sections from Human Renal Allografts: Results from the Banff Initiative for Quality Assurance in Transplantation (BIFQUIT) Trial

M Mengel, S Chan, J Climenhaga, H Regele, Y Kushner, R Colvin, P Randhawa. University of Alberta, Edmonton, Canada; University of Vienna, Vienna, Austria; MGH, Boston; University of Pittsburgh, Pittsburgh.

Background: The purpose of this study was to identify the best current immunochemistry (IHC) method for two critical diagnostic techniques in renal transplant, detection of C4d and BK virus.

Design: We conducted a multicenter trial of 60 labs using tissue microarray (TMA) sections of paraffin embedded kidney transplants with antibody-mediated rejection (AMR) and BK nephropathy. A nephrectomy with AMR was treated with different fixation protocols to test their influence on C4d results. Details regarding the lab-specific staining protocols were collected online. Locally stained TMA slides were returned for centralized panel scoring. Weighted kappa statistics comparing the panel reads were used to determine the inter-laboratory variability. For assessing the impact of different staining protocols, the 15 laboratories with the best reproducibility relative to a benchmark lab were compared to those 15 with the worst. The benchmark lab was identified by the review panel based on its outstanding performance.

Results: More than 80% of the labs used automated stainers. For C4d, the majority of top 15 labs applied heat-induced epitope retrieval using EDTA buffer at pH 8-9 on Ventana machines with a primary antibody dilution of <1:80 incubated for 20-40 minutes. Higher dilutions of the primary antibody were associated with worse reproducibility. Fixation <1h or fixation in ethanol had significant negative impact on inter-laboratory reproducibility. For BK, 70% used a monoclonal anti large-T-antigen antibody (PAb416) in a broad dilution range (1:40-1:5000). Those labs using different antibody clones or dilutions >1:100 had less reproducible results. No difference was found in regard to citrate or EDTA buffers for epitope retrieval. Those labs using microwave and/or retrieval times <30 minutes had less reproducible results. Polymer detection systems were superior to avidin-biotin based detection systems.

Conclusions: According to this quality assurance study, the optimal IHC technique for: C4d includes heat induced epitope retrieval, pH8-10, EDTA buffer, polyclonal antibody <1:80 for 20-40 minutes, and a polymer detection system. For BK stains, the optimal technique includes heat induced retrieval >30 minutes, either citrate or EDTA buffer, monoclonal antibody (PAb416) <1:100 for 25-35 minutes, and polymer detection system. Improved reproducibility should result from wider use of these protocols.

1682 Immunotactoid Glomerulopathy: Clinicopathologic Study of 16 Cases

SH Nasr, LD Cornell, ME Fidler, SS Sheikh, AA Amir, S Sethi. Mayo Clinic, Rochester, MN; Dhahran Health Center, Dhahran, Saudi Arabia.

Background: Immunotactoid glomerulopathy (IT) is a rare GN, tenfold rarer than fibrillary GN. To better define the clinicopathologic spectrum and prognosis of IT, we report the largest series to date.

Design: We identified 16 cases of IT from our pathology archives, between 1993-2011. All cases fulfilled the following diagnostic criteria of IT: glomerular deposition of microtubules that (*1*) had hollow centers at magnification of <30,000, (*2*) arranged in parallel arrays; and (*3*) stained with antisera to immunoglobulins by immunofluorescence (IF). Biopsies with clinicopathologic diagnoses of cryoglobulinemic GN or lupus nephritis were excluded.

Results: All 16 pts were Caucasians with a F:M ratio of 1 and a mean age at diagnosis of 60 yrs (range 41 to 80). Presentation included proteinuria (100%, mean 7.5 g/day), nephrotic syndrome (69%), renal insufficiency (50%, mean serum (S.) creatinine 2.0 mg/dL), and microhematuria (80%). 46% had hypocomplementemia. S. cryoglobulin and HCV antibody were negative. A S. M-spike was present in 63%. Hematologic malignancy was present in 38% of pts, including small lymphocytic leukemia (CLL) in 19%, lymphoplasmacytic lymphoma (LPL) in 12%, and smoldering myeloma in 12%. One pt had LPL and smoldering myeloma. The hematologic malignancy was discovered 1.8-6 yrs before IT diagnosis in 50% of pts and concomitantly with the IT diagnosis in the remaining 50%. The most common glomerular pattern on light microscopy (LM) was membranoproliferative GN (56%, including 31% with segmental membranous features) followed by global membranous GN (31%) and endocapillary proliferative GN (13%). Interstitial lymphomatous infiltration was present in all 19% of pts with CLL. By IF, 88% showed glomerular positivity for IgG, 25% IgM, and 6% IgA; the deposits were single light chain-restricted in 56%. On electron microscopy, the microtubular deposits were seen in the mesangium in 75% of cases, in the subepithelial space in 75% and in the subendothelial space in 75%. The mean microtubule diameter was 31 nm (range of means, 17-52). During a mean of 42 mo of follow-up for 13 pts with available data, 39% had complete or partial remission, 38% had persistent renal dysfunction, and 23% progressed to ESRD. Two-thirds of pts received immunosuppressive (IS) therapy.
Conclusions: IT typically affects older pts. Hematologic malignancy (most commonly CLL) is present in over a third of pts and a circulating paraprotein in two-thirds. LM usually shows membranoproliferative or membranous GN. Over a third of IT pts are expected to recover renal function with IS therapy.

1683 Endothelial Protein C Receptor Is Upregulated during Acute and Chronic Antibody-Mediated Rejection in Renal Allografts

T Nguyen, G Rizzuto, K-Y Jen, Z Laszik. University of California San Francisco, San Francisco, CA.

Background: Endothelial protein C receptor (EPCR) plays an active role in both pro-inflammatory and anti-inflammatory signaling mostly via protease activated receptors. Since endothelial cells are the primary target of antibody-mediated rejection (AMR), changes in endothelial expression of EPCR during AMR may have potential diagnostic and therapeutic utility. The aim of this study was to assess the endothelial expression of EPCR in acute and chronic antibody-mediated rejection in allograft kidneys.
Design: The study included renal transplant biopsies with acute AMR (n=6) (diffusely C4d positive) and chronic AMR with transplant glomerulopathy (n=6, diffusely C4d positive; n=7, C4d negative). Control cases included protocol biopsies 6 month post transplantation without any pathologic changes (n=10). Double immunofluorescence stains for CD34 and EPCR were performed on paraffin-embedded tissue. Co-expression of EPCR with CD34 in the renal cortex was assessed using computer assisted morphometric analysis.
Results: Expression of EPCR in the protocol biopsies was limited to the endothelial cells of large arteries and veins. EPCR expression was up-regulated in the tubulointerstitial capillaries of all three study groups including C4d negative chronic AMR ($p<0.0008$). There were no significant differences in endothelial EPCR expression between cases with C4d positive and C4d negative chronic AMR.
Conclusions: Up-regulation of EPCR in the tubulointerstitial capillaries during AMR may provide an additional marker to aid the morphologic diagnosis of various forms of AMR. Given the prominent role of EPCR in various signaling pathways, the possibility of EPCR as a therapeutic target should also be considered.

1684 Tubulointerstitial Nephritis in Common Variable Immunodeficiency

Y Raissian, SH Nasr, PJ Kurtin, S Sethi, TC Smyrk, LD Cornell. Mayo Clinic, Rochester, MN.

Background: Common variable immunodeficiency (CVID) is a primary immunodeficiency disorder characterized by decreased serum immunoglobulin levels and recurrent infections, and is often accompanied by autoimmune disease. Renal involvement in CVID has rarely been described and only in case reports. We describe a series of CVID patients (pts) with a characteristic tubulointerstitial nephritis (TIN).
Design: Renal biopsies from pts with CVID were identified from a database. Light microscopy, immunofluorescent (IF), immunohistochemical (IHC), and ultrastructural (EM) features were reviewed.
Results: Five cases of TIN in pts with CVID were identified. The mean age at biopsy was 33 yrs (range 14-58); F:M ratio was 2:3. All pts had an established diagnosis of CVID. Four pts underwent renal biopsy for acute or acute on chronic renal failure. The mean serum creatinine (SCr) was 4.1 mg/dl (range 0.8-8.0). Biopsies revealed a diffuse interstitial inflammatory cell infiltrate composed of many macrophages and lymphocytes with occasional eosinophils, plasma cells and neutrophils; and mononuclear cell tubulitis, along with mild to severe cortical interstitial fibrosis and tubular atrophy (10-75%). Two biopsies also showed focal non-necrotizing granulomatous inflammation. IHC revealed numerous CD68+ macrophages with a moderate number of CD3+ T cells and fewer scattered CD20+ B cells. Glomeruli and vessels showed no specific changes. IF was negative in the tubulointerstitial compartment and was negative or showed trace segmental granular capillary loop staining in glomeruli in 4 cases with IF studies performed; EM showed no specific features. Two pts had similar histologic findings in the lung, one of whom also had follicular and paracortical hyperplasia on a lymph node biopsy. Three pts had liver disease, one with panacinar hepatitis on biopsy, one with presumed cryptogenic cirrhosis, and one with cirrhosis presumed due to hepatitis C.
Follow-up data were available on 4 pts, at a mean of 44 months (range, 2-129) after the biopsy. Two pts were treated with corticosteroids and another with cidofovir for an unconfirmed viral infection. These 3 pts showed improved SCr but continued CRF (mean SCr 2.0 mg/dl, range 1.4-2.3). The fourth pt had end-stage renal disease at one month after presentation and required maintenance hemodialysis.
Conclusions: CVID should be added to the expanding list of systemic diseases associated with TIN. CVID-associated TIN is characterized histologically by increased interstitial macrophages and T cells, tubular atrophy, interstitial fibrosis, and sometimes non-necrotizing granulomas.

1685 The Banff Initiative on Quality Assurance in Transplantation: Immunohistochemistry for BK Virus in the Kidney

PS Randhawa, S Chan, J Climenhaga, G Zeng, H Regele, R Colvin, M Mengel. University of Pittsburgh, Pittsburgh, PA; University of Vienna, Vienna, Austria; Harvard Medical School, Boston, MA; University of Alberta, Edmonton, Canada.

Background: BK virus is an important pathogen in the kidney. Immunohistochemistry is the gold standard for diagnosis of BKV nephropathy, but its inter-laboratory reproducibility has not been evaluated.
Design: A tissue microarray(TMA) with 23 sample cores was constructed from nephrectomy specimens representing the full spectrum of BK infection from -VE to strongly +VE cases. This TMA allowed distribution of nearly identical sections to 81 participants at 60 centers. Each participating center stained the TMA using local protocols. Cases were categorized as 0, A, B or C based on staining intensity and 0, 1, 2 or 3 based on % of +ve tubular nuclei. BKV RNA was quantitated in separate samples of each tissue using real time PCR. Details of local staining protocols and evaluation scores of each participant were collected via an online survey. Stained slides were returned for centralized panel scoring. Weighted kappa (K) statistics were used to determine the inter-observer variability (comparison of local reads to panel scores) and inter-laboratory variability (comparison of panel reads on TMAs prepared at different centers).
Results: Participating centers generated a total of 2025 data points for analysis. Inter-observer reproducibility was substantial (mean kappa score (κ) = 0.64) However, using a reference case with the brightest staining, inter-laboratory reproducibility of the intensity of the stain and % nuclei was below chance (mean κ = -0.22), though it improved if only agreement on the % tubular staining was considered (κ = 0.29). Reproducibility for staining intensity remained poor, but improved (κ = 0.22) if it was based on the consensus reading for each case. Binary categorization of each biopsy as BKV positive or negative resulted in the highest agreement (mean κ = 0.77). BKV DNA content per cell increased progressively with increasing intensity of immunohistochemical staining (median BKV DNA per cell: 4.88E+01 in grade0, 5.82E+01 in grade A, 2.92E+04 in grade B, and 4.60E+04 in grade C). The threshold sensitivity of detection of immunohistochemistry was estimated to be 58.2 BKV genomic equivalents per cell.
Conclusions: There is good agreement between observers on the interpretation of a BKV stain, particularly if only the presence or absence of BKV is assessed. However, quantitative scoring of nuclear staining intensity, and percentage tubules infected as proposed in the Banff 2009 Conference on Allograft Pathology is not reproducible.

1686 The Significance of IgG4 Positive Plasma Cells in Renal Transplant Biopsies with Plasma Cell Rich Acute Cellular Rejection

G Rizzuto, T Nguyen, K-Y Jen, Z Laszik. UCSF, San Francisco, CA.

Background: Morphologic criteria have recently been established for IgG4-tubulointerstitial nephritis in native kidneys. However, no data are available about the potential existence and significance of IgG4-positive plasma cells following renal transplantation. Plasma cell rich acute cellular rejection (ACR) has a less favorable outcome than conventional ACR, the reasons for which are unclear. Here, we assess the IgG4 positive plasma cell load in transplant kidney biopsies with plasma cell rich ACR and also in cases with concurrent antibody-mediated rejection (ACR/AMR).
Design: Renal transplant biopsies were selected from computerized departmental files for the following study groups: plasma cell rich ACR (n=20), plasma cell rich ACR/AMR (n=7), control ACR (n=8), and control ACR/AMR (n=5). Only cases without concurrent glomerular or tubulointerstitial disease, other than acute rejection, were considered for the study. Immunofluorescent staining for IgG4, CD20, CD3, CD8, and CD68 were performed on formalin-fixed and paraffin-embedded tissues and cell density quantitatively assessed using computer-assisted morphometric analysis.
Results: Quantitative cell density analysis revealed a significant increase in IgG4 positive cells in plasma cell rich rejection biopsies compared to control biopsies ($p=0.002$), and the data support the potential existence of two subsets of IgG4 positive plasma cell rich rejection: IgG4-rich and IgG4-poor subsets. Overall, significantly fewer IgG4 positive cells were present in plasma cell rich ACR/AMR compared to plasma cell rich ACR alone ($p=0.04$). Statistically significant differences in B cell (CD20), T cell (CD3, CD8), and macrophage (CD68) density were not observed between the groups.
Conclusions: These findings establish the existence of an IgG4 plasma cell population in many, but not all, cases of plasma cell rich ACR. That IgG4 plasma cells are present in significantly fewer cases of plasma cell rich ACR/AMR suggest a possible pathogenic difference between pure ACR and ACR/AMR. Future work to correlate IgG4 positive plasma cell rejection, particularly IgG4-rich and IgG4-poor subsets, with clinical outcome is warranted.

1687 Progressing Amyloid Light Chain (AL) Deposits in the Kidney in Patients with Autologous Hematopoietic Stem Cell Transplant for Monoclonal Gammopathy

R Roth, T Nadasdy, A Satoskar, G Nadasdy, L Hebert, SV Brodsky. The Ohio State University, Columbus, OH.

Background: Systemic light chain (AL) amyloidosis is a condition in which the amyloid protein (amyloidogenic light chain) is abnormally deposited in the extracellular matrix of multiple organs/tissues in patients with monoclonal gammopathy. The mainstay of treatment for monoclonal gammopathy includes autologous hematopoietic stem cell

transplantation (AHSCT). The success of AHSCT is usually confirmed by the absence of monoclonal protein in the serum and urine. Amyloidosis progression is usually inhibited or reversed in patients after successful treatment.

Design: Herein, we present observations made on two patients who continued to develop progressive AL amyloidosis in the kidneys with worsening renal function despite the absence of monoclonal protein in the serum and urine after AHSCT for monoclonal gammopathy.

Results: For the first patient, kidney biopsies were performed before AHSCT and nine years after transplant. These two biopsies indicated progressive renal amyloid deposition. The renal biopsy of the second patient, performed three years after AHSCT, also showed severe amyloid deposits. Renal function was significantly deteriorating in both patients. For patient #1, serum creatinine was 1.40 mg/dl before stem cell transplantation and 3.05 mg/dl at the time of the second renal biopsy. For patient #2, serum creatinine was 2.00 mg/dl before the stem cell transplantation and 4.70 mg/dl at the time of the kidney biopsy. Numerous immunofixation and protein electrophoresis tests were negative for monoclonal protein both in serum and urine following transplantation, and both of these patients were considered to be in remission for their monoclonal gammopathy.

Conclusions: Progression of AL amyloidosis with no clinical signs of monoclonal gammopathy after successful AHSCT has not yet been described. Our findings indicate the possibility of a small population of neoplastic plasma cells persisting in patients following treatment. We hypothesize that the amount of monoclonal protein produced by these cells is miniscule and may not be detected by the current routine clinical tests. Close monitoring of the renal function and proteinuria as well as follow-up renal biopsies are warranted in patients who underwent AHSCT secondary to AL amyloidosis even in the absence of monoclonal protein by clinical tests. The clinicians involved in the care of patients with AL amyloidosis should be aware of this potential progression of AL amyloidosis in the kidney.

1688 Renal Amyloidosis: Origin and Pathology of 445 Recent Cases from a Single Center

SM Said, S Sethi, LD Cornell, ME Fidler, L Herrera Hernandez, JA Vrana, JD Theis, A Dogan, SH Nasr. Mayo Clinic, Rochester, MN.

Background: Amyloidosis is a rare disorder, characterized by extracellular accumulation of Congo-red-positive fibrillar deposits. The kidney is the most commonly affected organ by amyloidosis. The two most common types of renal amyloidosis are primary amyloidosis and secondary (AA) amyloidosis. Recently, several other types of amyloidosis have been recognized largely due to the introduction of mass spectrometry (MS) for amyloid typing.

Design: We reviewed the type and pathology of renal amyloidosis in all 445 cases diagnosed by renal biopsy from 2007-2011 at our pathology laboratory. Congo red stain was positive in all cases. Renal biopsies were evaluated by light microscopy, immunofluorescence (IF), and electron microscopy. The type of amyloid was determined by IF on frozen tissue, IF on pronase-digested paraffin tissue, immunohistochemistry, MS, and/or genetic testing.

Results: The type of amyloid was primary in 378 patients (84.9%), AA in 33 (7.4%), leukocyte chemotactic 2-associated amyloid (ALect2) in 13 (2.9%), fibrinogen A (AFib) in 5 (1.2%), Apolipoprotein in 3 (0.7%)(AApoAI in 1, AApoAII in 1, and AApoAIV in 1), combined AA and AL-AH in 1 (0.2%) and unclassified in 11 (2.4%)(mainly due to the lack of adequate tissue for IF and/or MS). The subtype of primary amyloidosis was AL in 357 of the 378 patients (94.4%; lambda (λ) in 81% and kappa (κ) in 19%), AL-AH in 15 (4%; IgGλ in 7, IgGκ in 2, IgAκ in 3, IgAλ in 1, IgMκ in 1, IgMλ in 1) and AH in 6 (1.6%, IgG in 5 and IgA in 1). Overall, MS was needed to determine the type of amyloid in 65 cases (15%). The mean age at diagnosis for all 445 patients was 63 yrs (63 for primary amyloidosis, 52 for AA, 66 for ALect2, and 56 for AFib), with a female to male ratio of 1.6. Amyloidosis involved glomeruli in 97% of cases (mesangium in 97% and basement membranes in 86%), vessels in 84%, interstitium in 58% and tubular basement membranes in 7%. ALect2 and AFib had a distinctive pattern of involvement: ALect2 was characterized by diffuse interstitial deposition, while AFib showed massive obliterative glomerular involvement.

Conclusions: With the advent of MS for amyloid typing, the type of renal amyloidosis can be determined in > 97% of cases. In our experience, primary amyloidosis accounts for 85% of cases. AL-AH (most frequently IgGλ) or AH (most commonly IgG) comprise 6% of cases of primary amyloidosis. AA, the distant second most common type of renal amyloidosis, is only 3-times more frequent than ALect2 and 6-times more than AFib. ALect2 should be suspected if there is extensive interstitial involvement and AFib if there is massive obliterative glomerular involvement.

1689 CD44 Staining Distingushes Focal-Segmental Glomerulosclerosis (FSGS) from Minimal Change Disease (MCD) in Pediatric Nephrotic Syndrome

W Sakr, X Zeng. Wayne State University, Detroit, MI.

Background: Beside MCD, FSGS is a significant cause of steroid resistant nephrotic syndrome in children. Distinguishes FSGS from MCD is based mainly on the detection of segmental sclerosis in glomerular capillary tuft. Because of the "focal" nature of FSGS, the segmental sclerosis may be missed by sampling error. No reliable biological marker for detecting FSGS is available currently. A body of evidence indicates that FSGS is caused by loss of podocytes, which have limited regenerative capacity. Parietal epithelial cells (PEC) have been proposed to be the stem cells and serve for transition to podocytes. CD44 is a glocoprotein involved in cell adhesion and migration thus a marker for functionally active PEC. Recent studies have been showed that CD44 staining is positive in recurrent FSGS in renal transplantation, but negative in MCD. The purpose of this study is to evaluate the value of CD44 staining in diagnosis of FSGS in pediatric patients with nephrotic syndrome.

Design: Pediatric patients who had "paired-biospy", initial at which diagnosis of "MCD" is established and then a follow-up biopsy due to steroid resistant nephrotic syndrome, with diagnosis of FSGS/MCD in Children's Hospital of Michigan during 2004-2010 were considered for our study. Immunohistochemistry staining for CD44 was performed on blank sections of paraffin blocks in each case. CD44 staining in PEC and podocytes were recorded as positive or negative.

Results: Seven patients had "paired-biopsy" in the study period and 4 patients had adequate tissue suitable for immunostaining. Neither PEC nor podocyte show CD44 staining in initial biospy in these 4 patients. In follow-up biospy, the CD44 staining in PEC is positive in FSGS patients (2/2, 100%) but negative in MCD. CD44 staining in podocyte was also detected in FSGS (2/2, 100%) and MCD (1/2, 50%).

		1st Bx		2nd Bx	
		Podo	PEC	Podo	PEC
MCD	Case1	0	0	0	0
	Case2	0	0	+	0
FSGS	Case3	0	0	+	+
	Case4	0	0	+	+

Conclusions: Our data suggest that CD44 staining in PEC is better than in podocyte for the assessing the risk of MCD to evolve to FSGS and may be a useful marker for distinguishing early FSGS from MCD. Study with large numbers are needed to support these observations.

1690 Diagnostic Value of Sox9 Staining To Identify Early Recurrence of Focal and Segmental Glomerulosclerosis (FSGS) after Renal Transplant

W Sakr, D Shi, X Zeng. Wayne State University, Detroit, MI.

Background: Recurrence of FSGS after renal transplant is present with proteinuria initially. Diagnosis of FSGS is made mainly by detection of segmental sclerosis in glomerular capillary tuft, an alteratin that is ofter "very focal and segmental" in early stage, therefore diagnosis can be missed due to sampling. Recent data suggest that FSGS is an irreversible podocyte injury by TGF-ß mediated apoptosis then fibrogenesis and sclerosis. Sox9 is a transcriptional factor and one of the downstream targets of TGF-ß. Previous reports indicate that Sox9 staining is pos in FSGS in segmental sclerotic and non-sclerotic glomeruli but lack of detailed information for its clinical use. The purpose of this study is to evaluate the value of Sox9 in diagnosis of early recurrence of FSGS post renal transplant.

Design: All patients who received renal transplant in Detroit Medical Center for a diagnosis of FSGS between 2004-2010 and who were clinically suspected to have recurrent FSGS based on proteinuria, and underwent multiple follow-up biopsies were included in this study. Immunohistochemistry staining for Sox9 on fixed tissues of all biopses was recorded as positive or negative. The relationship between Sox9 staining patterns and recurrence of FSGS were evaluated.

Results: Thirteen patients qualified during study period of whom 8 patients had 3 to 7 biopsies with adequate tissue for immunostaining. Pococyte is stained by Sox9 in FSGS case. Seven of 8 patients showd unique Sox9 staining (positive or negative) pattern through their multiple biopsy with/without FSGS. One patient had negative Sox9 staining in initially biopsy that turned positive in follow up biopsy demonstating FSGS. Figure 1 summarized the result of Sox9 staining in podocyte with 80% sensitivity and 66.7specificity. The positive and negative predictive value is 80% and 66.7% respectively.

	FSGS	No FSGS
Sox9 Pos	4	1
Sox9 Neg	1	2

No staining in PEC is noted.

Conclusions: Our data suggest that Sox9 staining in podocyte is a reliable marker for the detection of early recurrent of FSGS in renal allograft and have high sensitivity and positive predictive value, finding that need further comfirmation by studies with large number of patientis.

1691 Immunofluorescence Patterns in IgA Nephropathy and Their Significance

SN Salaria, MM Estrella, LJ Arend. Johns Hopkins University, Baltimore, MD.

Background: Immunoglobulin A nephropathy (IgAN), caused by glomerular IgA immune deposits, is the most common form of primary glomerulonephritis in the world. Prevalence of IgAN among racial groups, initial presentation, as well as progression of disease is highly variable. Diagnosis of IgAN relies on a combination of clinical history, light and electron microscopy, and direct immunofluorescence (IF) for immunoglobulins (Ig) and complements (C). Renal biopsy specimens are traditionally stained for IgA, IgM, IgG, C3, and C1q. Dominant or co-dominant IgA is considered diagnostic of IgAN, however, biopsies show a variety of IF patterns. The presence or absence of other Igs as well as complements may contribute to the pathology of IgAN.

Design: We reviewed IF staining in patients receiving an initial diagnosis of IgAN. We recorded Oxford classification scores as a measure of disease burden at the time of biopsy. This data was compared to the patient's demographics such as race, age, and gender; in addition, clinical parameters at the time of presentation were analyzed, including GFR and serum creatinine. Statistical significance was determined using T-test and Fisher's exact test.

Results: We identified 103 unique patients with a diagnosis of IgAN between 01/01/2000-09/24/2011. The median age of the patients was 35 years (3-82 years), 53% of the patients were male, 74% white, 13% black, 7% asian, 3% Hispanic, and 3% classified as other. Median creatinine at the time of diagnosis was 1.3 mg/dl (range 0.3-10.9). Mean GFR was 71 ml/min. The presence of C3 deposition in the biopsy correlated significantly with a higher mean GFR at diagnosis (73.2 with C3 vs 28.7 without C3; p 0.03), while C1q in the biopsy correlated with a lower GFR (40.7 with C1q vs 75.0 without C1q; p 0.01). Deposition of C1q was seen in 12% of the biopsies. There was no significant correlation between IgG and/or IgM deposition and GFR at diagnosis, but a trend toward higher GFR was seen with the presence of IgG or IgM alone as well as in combination. Comparing histologic scoring categories with Ig and C revealed a significant correlation between the presence of endocapillary proliferation and IgM deposition; in 78 biopsies with IgM deposits, 34 (44%) showed endothelial cell proliferation (E), versus 3 of 23 (13%; p 0.007) without IgM deposits with positive E score.

Conclusions: In conclusion, the presence of C1q deposition appears to correlate with lower renal function at the time of diagnosis of IgAN. Significantly, the presence of IgM was associated with more frequent endocapillary proliferation, a major risk factor for progressive renal failure in IgAN.

1692 Renal Biopsy Findings of Diabetic Nephropathy in Pediatric Patients with Type I Diabetes Mellitus

SP Salvatore, SV Seshan. Weill Cornell Medical College, New York City.

Background: Diabetic nephropathy (DN) occurs in 20-40% of type 1 diabetic patients with a prolonged natural course. Typically, the clinical symptoms of microalbuminuria, overt proteinuria and chronic renal insufficiency do not present until early adulthood, but in some pediatric patients, microalbuminuria or proteinuria may necessitate a renal biopsy.

Design: All native kidney biopsy records in our institution from 1995-2010 for pediatric patients, aged 17 and less, with clinical diabetes were reviewed. The pathologic features were classified (according to Tervaert et al JASN, 2010) and analyzed with clinical renal disease.

Results: Of the 6785 native kidney biopsies, 17 were pediatric diabetic patients, ranging from 10 to 17 years of age (mean 14) with a male:female ratio of 8:9. All patients had insulin dependent, type 1 diabetes, diagnosed from 4 to 12 years prior to the biopsy, mean 8 years. One 15 year old female had hypertension and one 12 year old male was on an ACE inhibitor. Three of the patients had poorly controlled diabetes, 2 with diabetic ketoacidosis. The clinical indication for biopsy was microalbuminuria in 7 patients, proteinuria in 7 (range: trace to 2.17g/day), hematuria in 1, and a decreased GFR in 2. The serum creatinine ranged from 0.3 to 0.9 mg/dL (mean 0.7). On biopsy, 16 of 17 showed diabetic glomerulopathy, Class I (isolated GBM thickening) in 5, Class IIa (mild diffuse mesangial (mes) expansion) in 8, Class IIb (marked diffuse mes expansion) in 1 and Class III (nodular mes expansion) in 1. Vascular sclerosis was seen in 9 patients: mild in 6 and moderate in 3. Arteriolar hyalinosis was present in 10. Four cases had superimposed glomerular disease, 1 IgAN, 1 post-infectious glomerulonephritis (PIGN), 1 membranous GN and 1 mes immune complex GN. Sixteen of the cases had minimal interstitial fibrosis (IF) and tubular atrophy (TA), from 0-20% (mean <5%), with one case of immune complex mes GN having 30%. Electron microscopy revealed GBM thickening, 375-1400nm (mean 675nm) with mes expansion in 10/16 (62.5%) and foot process effacement in 9 cases, ranging from 10-70%.

Conclusions: Pathological lesions of DN may be seen in a susceptible group of type I diabetic adolescents with microalbuminuria or frank proteinuria. These patients tend to have milder forms of DN, Class I to IIa glomerular lesions. Identification of parenchymal diabetic lesions may prompt more specific treatment strategies to potentially reverse or slow the progression of DN. Nearly ¼ of the cases were also found to have other renal diseases superimposed on features of DN.

1693 Collapsing Glomerulopathy in Advanced Diabetic Nephropathy

SP Salvatore, SV Seshan. Weill Cornell Medical College, New York City.

Background: Collapsing glomerulopathy (CG) is a pattern of severe podocytic injury which is rapidly progressive, presenting with massive proteinuria, and relatively resistant to therapy. Other associated etiologies include viral infections, drug therapy, autoimmune conditions, and in transplants with obliterative arteriopathy, previously proposed to be due to podocytic ischemic injury. Significant glomerular ischemia also occurs in cases of diabetic nephropathy (DN) with severe hyalin vascular disease.

Design: Of 4264 native kidney biopsies from our institution from 2003-2011, 534 (12.5%) had DN, and 26 of those (4.8%) had at least one glomerulus showing features of CG. Analysis of the clinicopathologic features of this cohort as well as immunohistochemical staining for vascular endothelial growth factor (VEGF) and podocytic markers WT1, synaptopodin, podocin, and beta-dystroglycan was performed.

Results: The 26 patients ranged in age from 26-80 years (mean 53), 14 male and 13 female. Most patients were type 2 diabetics (78%) with long-standing disease (mean 14 years), insulin dependent (67%), and hypertensive in 83%. Serum creatinine (Cr) levels were typically elevated, mean 3.75mg/dL (1.1-10.4), and had nephrotic range proteinuria, mean 9.8 g/d (2-29). Two patients had hepatitis C, none had HIV, autoimmune disease, or were on pamidronate or interferon. Renal biopsy showed segmental or global glomerulosclerosis (GS) in 2% (0-23) and 33% (0-80) of glomeruli, respectively. DN classification according to Tervaert et al (JASN 2010) was Class IV (>50% global GS) in 12 cases, III (nodular GS) in 8, IIb (severe diffuse mesangial (mes) sclerosis) in 4, and IIa (mild diffuse mes sclerosis) in 2. Segmental or global CG was present in 2-30% (mean 16%) of glomeruli, with 1 having 100% CG. Vascular disease was prominent, moderate in 44% and severe in 56%. Extensive arteriolar hyalinosis with >50% luminal stenosis in more than half of the arterioles was seen in 85.2% of cases. Markers of podocytic differentiation were lost in the glomeruli with CG for 100% synaptopodin and podocin, 75% beta-dystroglycan, and 70% WT-1. VEGF overexpression was seen in 43%. Follow-up on 12 patients: 9 (6 Class IV, 2 - III, 1 – IIb) developed chronic renal failure on average 9.7 months from the biopsy (0-36). The 3 remaining, 5 months to 2 years follow-up, had progressively increasing Cr with stable proteinuria.

Conclusions: CG contributes to the increased level or new onset of proteinuria in DN. Identification of CG in advanced DN with significant hyalin vascular disease is presumably due to podocytic ischemia and is of prognostic significance.

1694 Interstitial Eosinophilic Aggregates Is Distinctly More Common in Diabetic Nephropathy Than Other Glomerulopathies

K Sasaki, K Smith, R Nicosia, CE Alpers, B Najafian. University of Washington Medical Center, Seattle.

Background: The presence of interstitial eosinophilic aggregates (IEA) in renal biopsies is commonly interpreted as allergic type tubulointerstitial nephritis (TIN-A). However, in many cases, no significant correlation with a history of drug-use can be found. Here, we studied the prevalence of IEA in diabetic nephropathy (DN) as well as other common types of glomerulopathy.

Design: Diagnostic reports made by one pathologist between January 2010 and August 2011 were reviewed. The cases with DN (n=74) or other glomerulopathies including IgA nephropathy (IgAN) (n=43), membranous nephropathy (MN) (N=40), thrombotic microangiopathy (TMA) (n=14), amyloidosis (n=15), focal segmental glomerulosclerosis (FSGS) (n=121), membranoproliferative glomerulonephritis (MPGN) (n=10) were analyzed for the presence of IEA. A frequency of concurrent diagnosis among cases diagnosed as TIN-A (n=26) was also analyzed. Finally, demographics (age, sex, type1 vs type2 diabetes), and a history of antibiotics/NSAIDS use obtained from pathology requisition forms, and reported pathologic severity of mesangial expansion (advanced vs mild) were compared between cases of DN with (DN-IEA) and without (DN-nonIEA) concurrent IEA.

Results: Cases with DN have significantly higher frequency of concurrent IEA (27/74, 36%) compared with other glomerulopathies including IgAN (4/43, 9.3%, P<0.01), MN (5/40, 13%, P<0.01), TMA (0/14, 0%, P<0.01), amyloidosis (1/15, 0%, P<0.01), FSGS (19/121, 16%, P<0.001), and MPGN (0/10, 10%, P=0.02). Among cases with TIN-A, DN is the leading concurrent condition (13/26, 50%), followed by acute tubular injury (7/26, 27%), FSGS (4/26, 15%), other nonspecific chronic changes (3/26, 12%), IgAN (1/26, 3.8%), and MN (1/26, 3.8%). No significant difference was observed between DN-IEA and DN-nonIEA in age (55 yr vs 57 yr), sex, frequency of type I diabetes (8.3% vs 26.3%), antibiotic use (9.5% vs 16%), or NSAIDS use (30% vs 22%). DN-IEA shows significantly higher frequency of advanced mesangial expansion compared with DN-nonIEA (84% vs 60%, P=0.03).

Conclusions: IEA is a common concurrent finding in renal biopsies with DN. Correlations with the severity of glomerular changes suggest the probable link to the pathophysiology and natural history of DN. Correlations with other pathologic and clinical parameters are currently under further investigations.

1695 Staphyloccal Infection Associated Glomerulonephritis Mimicking Henoch-Schönlein Purpura

AA Satoskar, R Shim, S Brodsky, G Nadasdy, L Hebert, T Nadasdy. Ohio State University Medical Center, Columbus, OH.

Background: A patient with IgA dominant immune complex glomerulonephritis (GN) who presented with joint pain, petechial and bullous skin rash, and renal failure was treated with steroids and became septic. This prompted us to review our kidney biopsy material for Staphylococcus infection associated GN cases presenting clinically like HSP. Petechial rash has been described in patients with Stahylococcal infection related GN, but in the absence of known history of infection, this can be a diagnostic pitfall.

Design: We found 33 kidney biopsies from patients with culture proven Staphylococcus infection associated GN in our biopsy archives from 2005 to 2010. Seven of these had petechial skin rash.

Results:

Table 1

Patient	Diabetes	Infection	Organism	Blood culture	Creatinine at biopsy	Creatinine at follow up	C3 ; C4
1	present	leg ulcers, osteomyelitis	MRSA	Negative	9.7	dialysis	69 ; 30
2	present	leg ulcers	MRSA	Negative	4.5	dialysis	not known
3	absent	groin abscess	MSSA	Negative	4.6	dialysis	11 ; normal
4	absent	endocarditis	MRSA	Positive	2	2	104 ; 18
5	absent	skin wounds; motor vehicle accident	MRSA	Negative	1.9	dialysis	163 ; 25
6	absent	osteomyelitis	MSSA	Negative	2.8	1.3 improved	144 ; 24
7	absent	Abdominal wall abscess	MRSE	Positive	2.3	dialysis	169 ; 43

MRSE = methicillin resistant Staphylococcus epidermidis, MSSA=Methicillin sensitive Staphylococcus aureus

Patients ranged from 51 to 90 years of age. Acute renal failure, hematuria and proteinuria was the mode of presentation. Low complement levels were seen in only 2/7 patients. In 4 patients,infection was diagnosed only around the time of renal biopsy. In 3 patients, history of infection was known a few weeks before the biopsy. Followup period ranged from 1 to 8 months. Glomerular intracapillary proliferation, mild interstitial inflammation and red blood cell casts were the most common morphologic findings. Small crescents were seen in 2/7 biopsies. Interstitial fibrosis was prominent in 3/7 biopsies. Mesangial IgA and C3 were constant findings. Subepithelial humps were seen in two biopsies.

Conclusions: Staphylococcal infection associated IgA dominant glomerulonephritis can present with skin rash and therefore mimic HSP. A high index of suspicion for underlying Staphylococcal infection is warranted in adult patients with HSP-like presentation. Immunosuppressive treatment in such patients can induce sepsis. Blood cultures are frequently negative. Cultures from the site of infection are recommended. Renal outcome can be unpredictable.

1696 PAB597 – A Superior Agent for the Diagnosis of BK Virus Nephropathy When Compared to SV40

LE Schwartz, J Trofe-Clark, RD Bloom, V Van Deerlin, J Tomaszewski. Hospital of the University of Pennsylvania, Philadelphia, PA.

Background: BK virus nephropathy (BKVN) is a serious post-transplant complication that almost invariably leads to graft failure in kidney transplant recipients. The gold standard for diagnosis of BKVN is histologic examination of a kidney transplant biopsy. Molecular testing for BK virus (BKV) has emerged as a valuable screening tool and management guide for BKV infection and BKVN, but has not evolved to be the gold standard for diagnosis. In most institutions an SV40 immunohistochemical (IHC) stain and/or BKV in situ hybridization (ISH) is used as an ancillary study. In recent years we have adopted the use of PAB597 IHC, a novel monoclonal antibody directed against the VP-1 capsid protein (Bracamonte E, et al, Am J Transplant 2007;7:1552-1560) to assist in the diagnosis of BKVN. In this study, we report our institutional experience with the PAB597 IHC in the evaluation of kidney transplant patients for BKVN.

Design: After IRB approval, the kidney transplant files at our tertiary care hospital were retrospectively reviewed for patients diagnosed with BKVN between January 2004 and June 2011. We reviewed a Hemotoxylin & Eosin (H&E) stained slide, IHC stained slides for SV40 and PAB597 and, when available, BKV ISH for each patient. Data points included: types of BKV inclusions seen, nuclear staining counts for SV40, PAB597 and ISH, presence or absence of cytoplasmic staining, area of tissue sections analyzed, other histologic features, BKV polymerase chain reaction (PCR) results and selected clinical information.

Results: 22 patients with a biopsy confirmed diagnosis of BKVN and histologic material available for review were identified. All patients were noted to have type 1 and/or type 2 BKV inclusions on H&E. For all 22 patients, PAB597 IHC was noted to be positive with a mean of 21 nuclear labels (NL)/mm^2, whereas SV40 staining was negative for 8/22 (36%) patients (mean 12 NL/mm^2). BKV PCR data was available at time of biopsy for 8/22 (36%) patients with a mean viral load value of 5.9 log copies/mL, correlating to a mean PAB597 staining level of 6.27 NL/mm^2. BKV ISH was available and reviewed for 13 (59%) patients, and 12/13 showed positive staining (mean 22 NL/mm^2).

Conclusions: In our experience PAB597 is a superior single reagent for the phenotypic examination of BKVN as compared to SV40. If choosing a single reagent as an ancillary study for the evaluation of BKVN, our data indicates PAB597 to be the best choice.

1697 C3 Glomerulonephritis: Clinicopathologic Findings, Complement Abnormalities, Glomerular Proteomic Profile, Treatment and Follow-Up

S Sethi, FC Fervenza, JA Vrana, SH Nasr, Y Zhang, RJH Smith. Mayo Clinic, Rochester, MN; Carver College of Medicine, Iowa City, IA.

Background: C3 Glomerulonephritis (C3GN) is a recently described glomerulonephritis that results from dysregulation of the alternative pathway of complement (AP). In this study, we describe the clinical features, kidney biopsy findings, AP abnormalities, glomerular proteomic profile, treatment and follow-up in 14 cases of C3GN, two of which were recurrent in allografts following transplantation.

Design: The diagnostic criteria for C3GN were: Proliferative glomerulonephritis on light microscopy, bright C3 staining and the absence of Ig on immunofluorescence microscopy, and mesangial and subendothelial electron dense deposits and occasionally intramembranous and subepithelial deposits on electron microscopy (EM). Dense deposit disease was excuded based on EM.

Results: We found that C3GN affected all ages with equal sex predilection and typically presented with hematuria and proteinuria. In the majority of patients with native kidney disease, renal function remained stable, both in the short and long term. However, in the two patients with recurrent C3GN, recurrence occurred within one year of transplantation and resulted in decline in allograft function. Kidney biopsy showed a predominantly membranoproliferative GN, although both mesangial proliferative and diffuse proliferative GN were noted. The AP abnormalities were heterogeneous and were both acquired and genetic. The most common acquired abnormality was the presence of C3 nephritic factors, while the most common genetic finding was the presence of the Factor H H402 and V62 alleles. In addition to these risk factors, other abnormalities included Factor H autoantibodies and mutations in *CFH, CFI* and the *CFHR* genes. We also detected 3 novel *CFH* mutations that were not previously desccribed. Laser dissection and mass spectrometry of glomeruli from 8 C3GN patients and 1 DDD patient showed a similar proteomic profile with accumulation of proteins of the AP and terminal complement complex (TCC).

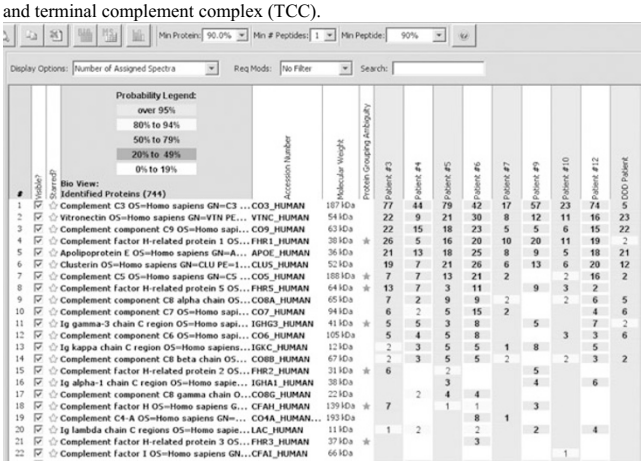

Conclusions: This study shows that C3GN is a disease associated with genetic and acquired abnormalities of the AP that lead to glomerular accumulation of AP and TCC proteins resulting in a complement-mediated proliferative GN.

1698 Prevalence of Leukocyte Chemotactic Factor-2 (LECT-2) in Renal Amyloidosis

S Sethi, AB Fogo, P Paueksakon. Mayo Clinic, Rochester, MN; Vanderbilt University, Nashville, TN.

Background: The type of amyloid whether AL, AA, hereditary or other has major impact on therapy. Amyloidosis may be identified by renal biopsy, but in some cases without definitive protein subtypes is not determined by standard immunofluorescence or immunohistochemistry. Recently, leukocyte chemotactic factor-2 (LECT-2)-associated amyloid has been described. We investigated the prevalence of this amyloid type contributing to previously unclassified cases.

Design: Forty-seven renal amyloidosis cases with available paraffin blocks in our 2002-2011 renal biopsy files at VUMC, were reviewed. Patients were designated as a classified amyloid (AA and AL) or a non-classified (absence of monoclonal staining pattern for kappa and lambda by IF and negative amyloid-associated protein IHC). IHC with LECT-2 specific antibody was performed. Mass spectrometry was performed in 8 patients.

Results: 43 patients had amyloid classified as either AL (42) or AA (1). These patients ranged from 33 to 84 years old (mean 62.1± 2.0) (pNS vs. non-classified), male/female ratio 1.8 and white/black ratio 9.8. Four patients had non-classified amyloid. These patients were 51 to 74 years old (mean 65.5±5.0), all males, and white/black ratio 3. Proteinuria was not significantly different (the non-classified 3.0 ± 1.0 g/24 h vs. 6.4± 0.7 in AA/AL). Two of 4 patients in the non-classified group were identified as amyloid LECT-2 by IHC and of these, LECT-2 was also identified by mass spectrometry in 1 patient. Two of 4 patients in the non-classified group were negative for LECT-2, however, the mass spectrometry showed apolipoprotein IV as a major protein component. Four of 43 AL amyloid patients showed positive LECT-2 IHC in glomeruli and arteries. However, LECT-2 was not identified by mass spectrometry in any of these 4 cases. The single patient with AA amyloid was negative for LECT-2 by IHC.

Conclusions: In summary, among 4 unclassified amyloidosis patients in our study, 2 had LECT-2 and 2 had apolipoprotein IV as a major protein component. Four AL patients also had LECT-2 as a minor protein component by IHC. Whether LECT-2 plays a pathogenic role in the amyloidogenesis in these AL patients will require further investigation. We conclude that positive IHC for LECT-2 may not be specific to determine amyloid type. Further, cases of unclassified amyloid by standard testing may include LECT-2 amyloidosis.

1699 Efficient Methods for Morphometric Analysis of Cortical Intersititial Volume Fraction in Protocol Kidney Transplant Biopsies

S Sharief, S Setty, S Akkina. Rush University, Chicago, IL; University of Illinois at Chicago, Chicago, IL.

Background: The use of the Banff criteria for scoring interstitial fibrosis in clinically stable kidney transplant recipients is problematic due to low degrees of fibrosis usually seen in protocol biopsies. For clinical studies, morphometric approaches such as point counting provide a more precise measure of fibrosis but at the expense of time. Our objective was to compare point counting with two computer-based methods of measurement of cortical interstitial volume fraction (Vvint).

Design: Ten randomly chosen protocol biopsies stained with Masson trichrome were scanned at high-resolution and then divided into individual images at 200X for quantitative analysis. Point counting was done using ImageJ software (NIH.gov) with a grid of 768 points. The point count within the interstitium excluding the Bowman's

capsule, tubular basement membranes, and blood vessels was enumerated and divided by the total number of points in the cortex to give the Vvint. For computer-based tools, we used ImageJ with the color deconvolution plugin and Histolab (Microvision Instruments, France). The ImageJ color deconvolution plugin was used to isolate the vector corresponding to the stain for fibrosis and then quantified using a threshold tool. For Histolab, areas of interest were selected by picking the color that corresponds to fibrosis, setting the threshold to account for slight variations in staining, and quantifying the selected area. Vvint, in all three methods, were averaged over all the images in each biopsy. We evaluated the level of agreement between methods using linear regression, correlation coefficients, and bias (computer methods - point counting). We also evaluated the relationship between measured Vvint, estimated glomerular filtration rate (eGFR), and Banff ci scores. Continuous data are reported as mean±standard deviation (SD).

Results: The average Banff ci score was 1.0±0.67 and average eGFR was 49.3±11.0mL/min/1.73m^2. The average Vvint by the point counting method was 9.9±5.4%. Table 1 shows the correlation between the computer-based methods and point counting. There were no significant correlations between eGFR and measured fibrosis.

Comparison of Computer-Based Methods to Point Counting

Method	r	R^2	Bias	SD
ImageJ	0.68	0.47	10.1	8.1
Histolab	0.91	0.84	3.21	4.9

Conclusions: Histolab showed much better agreement with point counting compared to ImageJ. Histolab may be an efficient method for measuring cortical interstitial volume fraction in protocol kidney transplant biopsies for clinical studies.

1700 Significance of Isolated Intimal Arteritis (v1) in Kidney Transplants: A Multicenter Observational Study

B Sis, S Bagnasco, B Lategan, M Haas, P Randhawa, L Cornell, A Magil, M Kuperman, A Herzenberg, K Sasaki, I Gibson, E Kraus. University of Alberta, Edmonton, Canada.

Background: Microarray studies of kidney transplant biopsies identified few isolated v-lesions (intimal arteritis) with no/minimal tubulointerstitial inflammation and low expression of T cell transcripts, questioning whether these cases reflect true rejection (AJT 2007).

We investigated the clinical significance of isolated v1 lesions in 266 kidney transplants performed between 1999 and 2010 in seven transplant centers in North America.

Design: We studied clinical parameters and graft survival (median follow-up after biopsy 44 months) in 100 isolated v1 biopsies (v1 and i<2 and t<2; group 1), in comparison to 90 biopsies with v1 plus high tubulointerstitial inflammation (v1 and i≥2 and t≥2; group 2) and 91 biopsies with v0 with minimal tubulointerstitial inflammation (v0 and i<2 and t<2; group 3). Biopsies with C4d positivity or from ABOi or cross-match positive kidneys were excluded. In selection of controls, no clinical parameter was matched (not to introduce bias). The biopsies were reviewed by a central pathology committee. Biopsies that met the aforementioned histopathology criteria and performed within 2 months of isolated v1 biopsies were selected as controls.

Results: Patient demographics and maintenance immunosuppresion were not different among study groups. The median post transplant time was 29 days in isolated v1, 33 days in group 2, and 21 days in group 3 biopsies (p>0.05). Indication for biopsies differed among groups: delayed or slow graft function triggered biopsies in 24% of isolated v1 group, but was uncommon in control groups (5% in group 2, 11% in group 3) (p<0.05). Acute deterioration of renal function triggered biopsies in 45% of isolated v1 group, 56% of group 2, and 44% of group 3. Serum creatinine at biopsy, 1 month and 6 month post biopsy did not differ among groups. Graft survival also did not differ among groups.

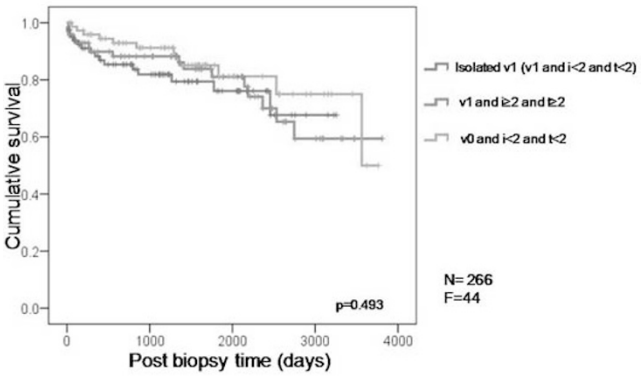

Conclusions: We conclude that, 1) isolated v1 biopsies are seen early and associated with delayed graft function; 2) v1 with or without high tubulointerstitial inflammation is not related to increased graft failure compared to v0. Thus, isolated v1 lesions, after the exclusion of antibody-mediated rejection, are of two types: T cell-mediated rejection and endothelial injury, and have no independent prognostic significance following anti-rejection treatment.

1701 JC Virus Infection in Renal Transplant Patients: Correlation with Urine Cytology, Molecular (PCR) Analysis and Clinical Findings

D Smith, C Chisholm, R Khode, K Walker, J Gildon, L Sayage-Rabie, A Rao. Scott and White Hospital, Temple, TX.

Background: Polyomavirus (BK and JC viruses) which are usually latent in the urothelium and renal epithelium can cause infections in immunosuppressed patients as also graft dysfunctions. Primary infection usually occurs at a young age and remains as a latent infection in greater than 90% of the adult population. Viral reactivation can be seen in immunocompromised individuals and can be detected by cytology as "decoy cells", immunohistochemistry, or by molecular methods. Reactivation of BKV in renal transplant recipients can result in BKV nephropathy and cause or simulate graft rejection. While much is known about BKV in renal transplant recipients, very few studies have examined the clinical implication of chronic infection with JCV in this population. The goals of this study are to determine the rate of JCV infection in renal transplant recipients, determine the sensitivity and specificity of decoy cells with respect to molecular assay, and to identify clinical and laboratory manifestations associated with JCV infection.

Design: Over a four month period, urines submitted for BKV/JCV PCR from patients status post renal transplant were included. Specimens were assayed by PCR and cytology. For molecular testing, DNA was extracted from urine using Biomerieux EasyMag and assayed using FOCUS Diagnostics BK and JC virus assays. For cytologic studies, Thinprep slides were prepared from urine specimens which were positive for JCV along with 36 that were negative.

Results: Over a four month period, the urines of 281 renal transplant patients were submitted for BKV/JCV molecular testing. 101 were positive for BKV, 20 JCV, and 7 for BKV and JCV. Median time to JC infection following transplant was 64 days. JC viral load ranged from 3.6 log (10) to greater than 7 log (10) copies/ml. The mean BUN and creatinine was 1.42 mg/dl and 23 mg/dl, respectively. Acute rejection was not observed in any patients infected with JCV. The sensitivity and specificity of decoy cells in diagnosing JCV is 30% and 97%, respectively, with positive and negative predictive values of 86% and 71%, respectively. The presence of decoy cells was not related to viral load or viral co-infection.

Conclusions: Urine cytology and decoy cell identification may not represent an optimal screening tool for JCV infection and the presence of decoy cells does not correlate with viral load or BKV co-infection. The incidence of JCV infection in renal transplant patients is low compared to that of BKV. Unlike BKV in this patient population, JCV is not associated with specific acute clinical or laboratory finding.

1702 Renal Allograft Biopsy Inflammatory Cell Quantitation Using Image Analysis Algorithms: Correlation with Pathologist Assessment and Rejection Severity

GH Smith, J Kong, AB Farris. Emory University, Atlanta, GA.

Background: Pathologists and clinicians often rely on assessment of inflammatory cell infiltrates in renal allograft biopsies when diagnosing rejection and grading the rejection process. Slight histologic variations can make big differences in the subsequent treatment course for patients. However, prior studies have shown limited reproducibility in such evaluations. We tested the utility of immunohistochemistry (IHC) image analysis in assisting with these designations.

Design: Whole slide images were obtained in a cohort of 58 renal biopsies containing allograft rejection, a borderline pattern, polyomavirus nephritis, normal donor tissue, and stable allografts for a variety of stains. CD3 stains were quantitated using a positive nuclear IHC algorithm tuned to detect CD3+ cells (Fig 1). The CD3+ cell density was compared with (a) pathologist assessment of percent inflammatory cell infiltrate on routine slides, (b) diagnosis, and (c) other parameters such as creatinine.

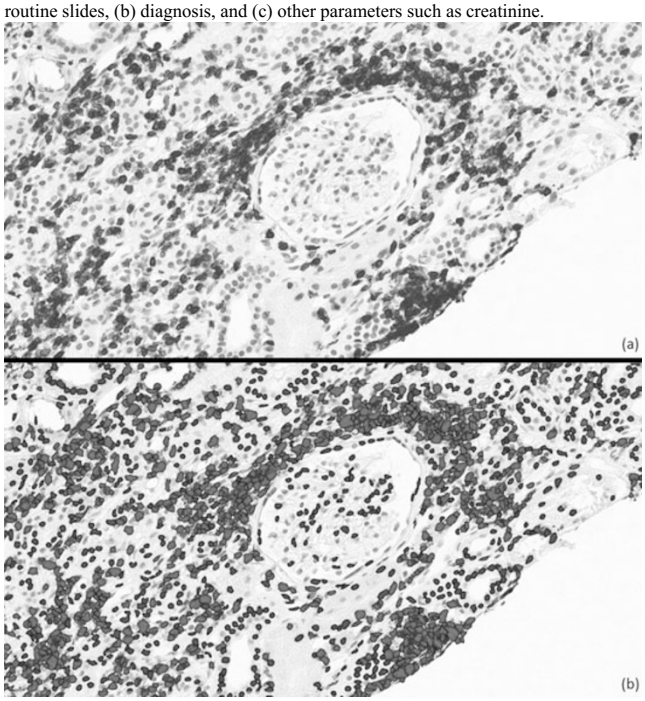

Fig 1. (a) IHC stained CD3+ inflammatory cells in the renal interstitium are brown. (b) Image analysis algorithm detects and quantitates CD3+ cells (red) and CD3- cells (blue).

Results: By linear correlation, the computed CD3+ cell density (# of CD3+ cells/mm^2) showed a direct correlation with the pathologist assessment of percent inflammatory infiltrate (R^2=0.48, P<0.0001) and with creatinine (R^2=0.50, P=0.0022) (Fig 2). Considering cases with acute cellular rejection (ACR), CD3+ cell density increased from borderline (531), to ACR1A (673), to ACR1B (1,336).

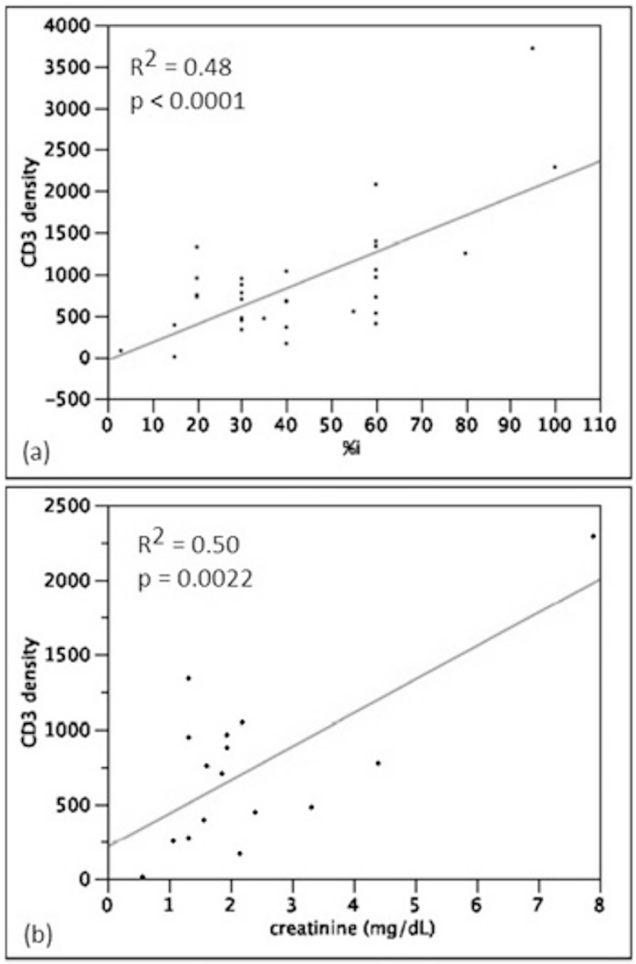

Fig 2. (a) CD3+ cell density versus pathologist assessment of percent inflammatory infiltrate (%i). (b) CD3+ cell density versus creatinine.

Conclusions: The cell counting algorithm showed correlations with the pathologist assessment of inflammatory infiltrate as well as creatinine, suggesting its promise in assessing renal allograft biopsies, analogous to flow cytometry on a slide.

1703 Anatomy of the [Non Kimmelstiel-Wilson Nodule (KWN)] Segmental Mesangial Expansion (SME) in Diabetic Glomeruli

LC Stout. University of Texas Medicall Branch, Galveston, TX.

Background: SMEs occurred in the same location in the glomerulus as KWNs, but differed in that the expanded mesangium was morphologically normal and admixed with mesangial nuclei and vascular spaces. This study describes their 3 dimensional structure using 4 µm paraffin step serial sections in 10 diabetic cases, and 1 µm plastic serial sections in 1 of the cases.

Design: The study population consisted of 74 diabetics and 59 matched controls retrieved from consecutive autopsies at our hospital. Twenty five of the diabetics with any degree of diabetic glomerular change ranging from minimal to severe (end stage cases were omitted) were studied with 18 4 µm serial sections stained as follows: periodic acid-Schiff (PAS), IgG, IgM, Jones' periodic acid-methenamine silver (PAM), Masson's trichrome, IgA, albumin, lysozyme, PAS, fibrinogen, fibronectin, PAM, trichrome, kappa light chains, lambda light chains, leukocyte common antigen, PAS, and smooth muscle actin. SMEs >40 µm were traced through the 4 µm sections starting with PAS 9 in 102-108 glomeruli per case in 10 of the 25 diabetics with minimal to mild changes. They were traced through 1 µm PolyBed 812 embedded toluidine blue stained serial sections in 3 complete glomeruli in 1 of the cases.

Results: In the 4 µm sections 6/10 cases had 19 (1-7) SMEs that were 30 x 40 to 60 x 70µm in area and occupied 3 to 9 levels. The SME mesangium was reticular, contained mesangial/endothelial nuclei, and vascular spaces without glomerular capillary basement membranes (GBMs) that eventually opened into capillaries at the SME periphery. SMEs arose at capillary branch points, with the involved capillaries having no or partial GBMs. In the 1 µm sections 3 glomeruli from 1 case had 6 SMEs, 2 of which were fed by an afferent arteriolar branch (AAB) with complete mesangial interposition (MI). MI was confirmed by electron microscopy in another AAB, and the 1 µm sections confirmed the absence of GBMs in intra-SME vascular spaces, some of which were as tiny as the SME reticular spaces. Most intra SME vascular spaces could be traced from feeding to peripheral or peripheral to peripheral capillaries.

Conclusions: The little known SMEs are large mesangial proliferations that appear capable of reducing free capillary filtration surfaces and increasing mesangial-capillary surfaces. The presence of MI in some feeding capillaries, the origin of SMEs at branch points, and the apparently normal SME mesangium suggests that SMEs may be a reaction to increased glomerular capillary flow/pressure.

1704 Molecular Expression of Podocytes in the Variants of Focal Segmental Glomerulosclerosis

LA Testagrossa, R Azevedo Neto, V Woronik, DMAC Malheiros. Hospital das Clinicas da Faculdade de Medicina da USP, Sao Paulo, SP, Brazil; Faculdade de Medicina da USP, Sao Paulo, SP, Brazil.

Background: Focal segmental glomerulosclerosis (FSGS) is the most prevalent primary glomerulopathy in Brazil and its incidence is increasing worldwide. Primary FSGS is characterized clinically by affecting young people and causing severe proteinuria and nephrotic syndrome. The pathogenesis is related to podocyte injury, which may be due to several factors: viruses, drugs, immunological, etc. In 2004, the Columbia classification of FSGS identified five histological variants of the disease: collapsing (COL), usual (NOS), tip lesion (TIP), perihilar (PHI) and cellular variant (CEL). Several studies have demonstrated molecular changes in podocytes of FSGS patients, which were observed in molecules involved in the filtering and structural function of these cells like nephrin, podocina, CD2AP, α-actinin-4, synaptopodin, etc. as well as in molecules of podocyte differentiation like CD10, WT-1, and of cell division: Ki-67 and PCNA. The objective of this study was to classify the FSGS biopsies according to the Columbia classification and to analyze the occurrence of molecular changes on these variants.

Design: 131 cases of renal biopsies with a diagnosis of primary FSGS in the period 1996 to 2006 were classified in COL, NOS, TIP, PHI and CEL, and then stained with immunohistochemical reactions to the primary antibodies: CD10, WT-1, Vimentin, Synaptopodin, α-actinin-4, GLEPP-1, cytokeratin 8-18, cytokeratin 19, and Ki-67.

Results: FSGS classification resulted in 38.2% of NOS variant, 36.6% COL, 14.5% TIP, 6.9% PHI and 3.8% CEL. The podocytes of COL variant biopsies were distinguished from the other variants for having lost the expression of CD10 (p<0,01), WT-1 (p<0,01) and α-actinin-4 (p <0,05) in podocytes. Furthermore, they gained expression of the cytokeratin 8-18 (p <0.05) and 19 (p <0.01). The group of CEL and COL variants differed from the group pf other variants regarding the expression of cell division marker Ki-67 in podocytes (p <0.05).

Conclusions: COL variant of FSGS presents molecular changes in podocytes that differs from other variants and can be demonstrated by immunohistochemistry. The differential diagnosis of this variant is important because of the worse clinical outcome in comparison with TIP, NOS, PHI and CEL variants, so the identification of these markers by immunohistochemical may be useful in the diagnosis on the routine practice and also for the better compreention of the disease.

1705 Assessing Graft Rejection by Automated C4d and CD34 Quantitation and Co-Localization

JE Tomaszewski, T Baradet, CC Hoyt, JR Mansfield, M Feldman. University of Pennsylvania Health System, Pennsylvania, PA; Caliper Life Sciences, Hopkinton, MA.

Background: Rejection is the major cause of graft failure, and if the injury to the organ is severe, it may not recover; prompt diagnosis of acute rejection is therefore important, with the monitoring of capillary C4d deposition being a reliable early indicator of humeral rejection. For renal biopsies in particular, testing requires taking two biopsies, one for frozen-section analysis with immunofluorescence (IF) and the other for formalin fixation and visual assessment with histochemical stains. IF labeling is not often used for formalin-fixed, paraffin-embedded (FFPE) renal specimens because of its inherent autofluorescence, which makes IF imaging and marker quantitation difficult. Spectral imaging can overcome autofluorescence interference, enabling the use of FFPE sections for renal imaging. Vessels in graft sections can fluorescently labeled for CD34 and C4d and then automated morphology-based image analysis and quantitation can be used to obtain an objective assessment of rejection.

Design: A cohort of matched formalin-fixed and frozen renal biopsy specimens were sectioned and stained for CD34 and C4d, and IF images of them acquired using a spectral imaging system. These were analyzed using an automated morphologic image analysis software package to assess C4d staining levels in capillaries. An objective measure of rejection status was then developed using a trainable pattern-recognition-based image analysis tool. This automatically identifies capillaries and measures C4d in capillary walls and immediately surrounding the capillaries. Automated measures were compared to visual assessments.

Results: Autofluorescence-free IF images from FFPE specimens were obtained using spectral imaging. Automated morphologic analysis of the images identified vessels and quantified the C4d intensities within those regions. Results from FFPE specimens were comparable to those from frozen, and the image-based objective measure of rejection status gave good correlation to visual assessment.

Conclusions: Automated quantitation of dual-labeled (CD34 and C4d) FFPE renal biopsy specimens can be achieved using spectral imaging and morphologic image analysis software, and gives a good correlation with results from frozen sections and against visual assessment. This methodology shows promise for becoming a routine method for clinical assessment of organ transplant biopsies and is amenable to studies of archival tissue.

1706 Pathological Characteristics of the Kidney and Bone of Patients with Itai-Itai Disease (Chronic Cadmium Toxicity)

K Tsuneyama, M Yazaki, T Minamisaka, K Nagata, H Baba, T Tsuda, K Aoshima. University of Toyama, Toyama, Japan; Hagino Hospital, Toyama, Japan.

Background: Itai-itai disease (IID), which is recognized in Japan as a pollution-related illness, is caused by chronic exposure to the mineral cadmium (Cd). Excess Cd accumulation in the proximal renal tubules (PRT) causes renal atrophy and secondary osteomalacia. In the present study, we assessed kidney and bone specimens of IID patients and compared the degree of histopathological change in these specimens with Cd concentrations within organs.

Design: Autopsy specimens from 71 IID patients and 27 patients not exposed to Cd pollution were examined. Cd concentration was measured using fresh organs. H&E staining was performed in addition to specialized staining with Azan for detecting fibrosis, Yoshiki staining for osteoid recognition, and immunostaining for metallothionein (MT), which binds and detoxifies Cd, CD10, a marker of the PRT, and EMA, a marker of the distal renal tubules (DRT). Images were analyzed with WinRoof. Statistical analyses were performed using JMP.
Results: Cd accumulation in the organs of the IID patients was 5.2 (liver), 4.1 (pancreas), 4.9 (thyroid gland), 7.3 (muscle), 3.3 (rib), 0.38 (renal cortex), and 0.62 (renal medulla) times higher than that of the controls. More than 80% of the IID patients showed kidney atrophy, with the surface of the kidney having a sandpaper-like surface. Microscopically, marked atrophy of the PRT and interstitial fibrosis with inflammatory changes were commonly observed among the IID patients, but there was less damage to the DRT. The intensity and distribution of MT in the kidneys of the IID patients were weaker than those of the controls. In bone, severe osteomalacia was observed in all of the IID patients before their deaths and was diagnosed by X-ray. However, more than 80% of these patients had mild-to-moderate osteomalacia in remission at autopsy. The degree of renal damage and osteomalacia was not related to the Cd concentration.
Conclusions: Atrophy of the PRT with interstitial changes was commonly observed among the IID patients. Renal damage may be a primary event and intractable to treatment. In contrast, osteomalacia was improved in most of the IID patients because of recent progress in treatments. The volumes of MT and Cd were markedly reduced in the kidneys of the IID patients. A portion of the excess Cd may have moved to other organs. However, we hypothesized that a portion of the excess Cd may have spilled into the urine due to renal damage. Examination of urinal Cd concentration should be required as part of a medical check-up of residents in Cd-polluted areas.

1707 Renal Glomerular and Tubular Specific Gene Expression Profiles from Laser Capture Microdissected Mouse Kidneys

S Tzeggai, J Pearcey, B Sis. University of Alberta, Edmonton, Canada.
Background: The kidneys serve several homeostatic functions including blood filtration and removal of wastes. The kidney is an anatomically complex organ composed of various distinct cell types and histological compartments. To gain understanding of molecular regulations in renal compartments, we established a method to isolate high-quality RNA from glomeruli and tubules of kidneys. We aimed at identifying glomerular-specific and tubular-specific genome-wide gene expression profiles.
Design: Three normal CBA mouse kidneys were cut at 7 μm thickness onto membrane slides using a cryostat and stained with H&E. We performed IR/UV laser capture microdissection to isolate glomeruli and cortical tubules from whole microscopic kidney sections. After microdissection, total RNA was extracted using the PicoPure RNA Isolation Kit. RNA quality and quantity were then measured using Agilent RNA 6000 Pico Kit and the Quant-iT RiboGreen method, respectively. Glomerular and tubular RNA samples were amplified with the RiboAmp HS PLUS Amplification Kit. Measurement of large-scale gene expression was done using Affymetrix mouse 430 2.0 microarrays.
Results: Pools of three replicates of 80 glomeruli and 80 tubules from 3 different kidneys yielded high RNA quality and quantity. We obtained a mean 79 μg and 51 μg of antisense RNA from microdissected glomeruli and tubules, respectively, after two amplification rounds of approximately 1 ng of input total RNA. Thus we obtained sufficient amounts antisense RNA to run Affymetrix microarrays. A class comparison between microdissected glomeruli and tubules showed a total of 5953 differentially expressed genes, of which 2878 genes with a prominent selective expression in the glomeruli. The glomerular and tubular selective gene lists included numerous novel genes in addition to genes with "a priori" known glomerular and tubular expression.
Conclusions: A systemic analysis of glomerular and tubular specific gene lists allows discovery of novel transcripts and pathways involved in molecular regulation of glomerular and tubular functions in the kidney.

1708 Intrarenal Bile Casts in Hepatorenal Syndrome: A Common and Underrecognized Finding

CM van Slambrouck, SM Meehan, A Chang. The University of Chicago Medical Center, Chicago, IL.
Background: Acute renal failure is a common complication of severe liver injury, however the mechanisms are poorly understood. Bile nephrosis (also termed cholemic nephrosis) is characterized by the presence of intratubular bile casts and is rarely reported in jaundiced patients with liver dysfunction. We hypothesized that bile nephrosis could be a major cause of acute renal failure in this clinical setting. Therefore, we conducted this study to determine the prevalence and characteristics of intrarenal bile casts in patients with hepatorenal syndrome, which represents a severe subset of patients with liver failure.
Design: Archival paraffin embedded autopsies of all 13 patients with hepatorenal syndrome over a 7-year period were examined for the presence, extent, location, and characteristics of intratubular bile casts. Bile casts were confirmed with a Hall's stain. A Prussian blue iron stain was used to exclude the presence of hemoglobin casts. Histopathologic findings were correlated with relevant clinical and laboratory data.
Results: The mean age of the 13 hepatorenal syndrome patients was 53.5 years, with 7 males and 6 females. Intratubular bile casts were present in 7/13 of cases. Patients with few casts had mainly distal nephron involvement. In some severe cases (3/7), there was bile cast extension into more proximal nephron segments. Acute tubular injury (ATI) was present in 8/13, negative in 2/13, and indeterminate from autolysis in 3/13 cases. ATI was more frequent in patients with bile casts 5/13 versus those without 3/13. There was a trend toward higher total bilirubin (22.4 vs 14.2 mg/dL) and lower albumin (2.9 vs 3.7 g/dL) in patients with bile casts. Interestingly, patients with alcoholic cirrhosis may be more prone to tubular bile cast formation.

Cirrhosis Etiology and Bile Casts

Cirrhosis	Bile Casts	No Bile Casts
EtOH	4	0
EtOH / HepC	1	1
HepC	0	3
Other	2	2

Intratubular bile casts are acellular, have a pigmented yellow-green appearance on H&E and must be distinguished from bile tinged casts of sloughed epithelium, calcium oxalate, and Tamm-Horsfall protein.
Conclusions: Bile casts are present in a majority of hepatorenal syndrome patients at autopsy. In this clinical setting ATI is more frequent in patients with bile casts. This common finding is often not recognized and may represent an important contribution to renal dysfunction in this clinical setting through direct toxicity to the tubular epithelium, obstruction, or both. Additional studies need to be performed to determine whether the etiology of liver disease may predispose some patients to bile cast nephropathy.

1709 C1q in the Donor Kidney: A New Form of C1q Nephropathy

AM Wright, S Patel, A Gaber, R Barrios, L Gaber, L Truong. The Methodist Hospital, Houston, TX.
Background: C1q glomerular deposition has been described in C1q nephropathy, subsets of traditionally classified glomerulonephritis, otherwise unclassifiable glomerulonephritis, and in renal biopsies for asymptomatic hematuria or proteinuria. This controversial classification is compounded by a lack of knowledge on C1q glomerular deposition in the general population.
Design: A total of 356 post-perfusion kidney donor biopsies between 2008-2011 were reviewed to assess the frequency of C1 glomerular deposition and its significance. The intensity (0-3+) and distribution (focal, segmental, global, diffuse, mesangial, peripheral) of C1q glomerular deposition were recorded by three independent observers and biopsies with at least focal segmental 1+ staining were correlated with staining of IgG, IgA, IgM, C3, C4, kappa/lambda light chains, donors' information and graft outcome.
Results: C1q glomerular deposition was noted in 17/356 biopsies (4.8%). Clinical data included: 14 deceased donors, 3 living donors, 4 females, 13 males, ages 16-62 years, 8 Caucasian, 9 Hispanic, 5 with hypertension, 1 diabetic, and 2 with extended donor criteria. Features of C1q glomerular deposition in the 17 biopsies included: 17 mesangial; 0 peripheral; average intensity 1.5+; 0 as an isolated finding; 4 with IgG (1.1+); 8 with IgA (1.6+); 16 with IgM (1.6+); 14 with C3 (1.6+); 1 with C4 (1+); 5 with kappa light chain (1.2+); and 5 with lambda light chain (1.6+). Electron microscopy was performed in 3 biopsies and showed mesangial electron dense deposits in each. Light microscopy showed no changes in 4, tubular atrophy/interstitial fibrosis in 7 (mean cortical surface area involvement 10.4%), mesangial hypercellularity in 6, enlarged glomerular size in 4, and enlarged urinary space in 4. Vascular intimal sclerosis was mild to moderate in 10 and not present in 7. Follow-up biopsies were done in 3 patients (0.5-2 months post-transplant): 1 had no change in IF staining pattern, 1 had complete loss of IF staining, and 1 had acute antibody-mediated rejection. One patient had 2 follow-up biopsies done (5 months and 1 year post-transplant) and showed loss of C1q staining, but progression of tubular atrophy/interstitial fibrosis of unknown etiology.
Conclusions: C1q glomerular deposition can be seen in the general population. This finding expands the spectrum of glomerular diseases characterized by C1q glomerular deposition. C1q glomerular deposition may disappear after transplantation and does not seem to adversely affect the short-term outcome of the renal transplant.

1710 Absence of PAI-1 Results in Direct Podocyte Protection In Vivo

H-C Yang, A Morden, I Pastan, T Matsusaka, I Ichikawa, AB Fogo. Vanderbilt University Medical Center, Nashville, TN; Florida State University, Tallahassee, FL; National Cancer Institute, Bethesda, MD; Tokai University Medical School, Isehara, Kanagawa, Japan.
Background: Plasminogen activator inhibitor-1 (PAI-1) inhibits serine protease activity and directly modulates cell migration. Our previous data *in vitro* and in the 5/6 nephrectomy model suggests PAI-1 has direct impact on podocytes. To test our hypothesis that absence of PAI-1 protects against direct podocyte injury *in vivo*, we bred *PAI-1*$^{-/-}$ mice with NEP 25 mice, in which podocytes express human CD25 receptor under the nephrin promoter, and are selectively injured by injecting immunotoxin (LMB2) that binds to this receptor.
Design: *PAI-1*$^{-/-}$/Nep 25 mice (n=10) and *PAI-1*$^{+/+}$/ Nep 25 mice (n=8) were exposed to LMB2 toxin (mean dose 11 ng/g BW, i.p.). Mice were sacrificed at day 10 and glomeruli were isolated. Urine total protein/creatinine ratio, glomerulosclerosis index (0-4 scale), podocyte number and differentiation markers were measured.
Results: PAI-1 deficiency did not have any effect on blood pressure; however, kidney function was improved as indicated by the lower body weight (*PAI-1*$^{-/-}$ 25.78±0.94 *vs.* WT 30.63±0.10 g, $p<0.05$), which implied less edema. *PAI-1*$^{-/-}$ mice had initial increased proteinuria that then returned to WT level. Podocytes were preserved more in *PAI-1*$^{-/-}$ mice as indicated by increased WT-1 (*PAI-1*$^{-/-}$ 5.21±0.23 *vs.* WT 4.02±0.25 WT-1 positive cells/glom, $p<0.05$). This data and the increased expression of GLEPP-1 (*PAI-1*$^{-/-}$ 2.43±0.52 *vs.* WT 1.13±0.22, $p<0.05$) and synaptopodin (*PAI-1*$^{-/-}$ 2.23±0.30 *vs.* WT 1.28±0.30, $p<0.05$) in *PAI-1*$^{-/-}$ mice demonstrate that knocking out the PAI-1 gene provided increased podocyte protection against direct immunotoxic injury. The glomerulosclerosis index was also numerically lower, suggesting that *PAI-1*$^{-/-}$ protected against renal injury after direct podocyte injury (*PAI-1*$^{-/-}$ 2.12±0.14 *vs.* WT 2.42±0.15, $p>0.05$). The greater expression of glomerular collagen-I mRNA (*PAI-1*$^{-/-}$ 3.76±1.05 *vs.* WT 1.24±0.30, $p<0.05$), despite less glomerulosclerosis suggests degradation or post-transcriptional modification of the collagen protein.
Conclusions: Our data suggest that the absence of PAI-1 protects podocytes by preserving podocyte number and differentiation markers after toxic injury which leads to improved outcomes of progressive kidney disease.

1711 Facilitation of Renal Allograft Biopsy Evaluation by Using Combined CD3 and PAS Special Stains

Z Yu, J Frazier, WF Kern, M Turman. University of Oklahoma, Oklahoma City, OK.

Background: Renal biopsy plays an important role in transplant allograft management. Based on the mechanisms causing allograft injury, renal transplant rejection can be roughly divided into two categories, antibody-mediated rejection and T-cell-mediated rejection. The diagnosis of T-cell-mediated rejection is based on the observation of tubulitis, arteritis, and interstitial lymphocytic infiltrates. Most laboratories use routine H&E and PAS stains to evaluate these inflammations. However, assessment sometimes can be difficult and may be not accurate when the cellular rejection is complicated by other renal injuries. Some pathologists utilize CD3, a pan T-cell marker, immunohistochemical stain (IHC) to help identify the T-lymphocytic infiltrates. However, routine IHC is usually performed without a counterstain which gives an indistinguishable background so that one cannot readily determine the location of the T-lymphocytic infiltrates, i.e., on the tubular epithelium (tubulitis) or merely in the interstitium. To resolve this issue, we developed a method that uses combined CD3 and PAS special stains.

Design: 10 previous transplant renal biopsy cases were selected for method validation. All subsequent transplant renal biopsies (more than 30 cases) were tested for the new combined CD3 and PAS method. Formalin-fixed paraffin-embedded tissue blocks were cut at 2 μm thick and embedded on positive charged slides. The slides were first stained with anti-CD3 polyclonal antibody, and then stained with PAS. The entire procedure was performed using Ventana automated system and took about 3 to 4 hours.

Results: In comparison to routine PAS stain alone or CD3 IHC without counterstain, the combined CD3 and PAS method clearly highlights the location and the intensity of the T-lymphocytic infiltrates; thus it has significantly facilitated our ability to evaluate T-cell mediated rejection in renal allografts.

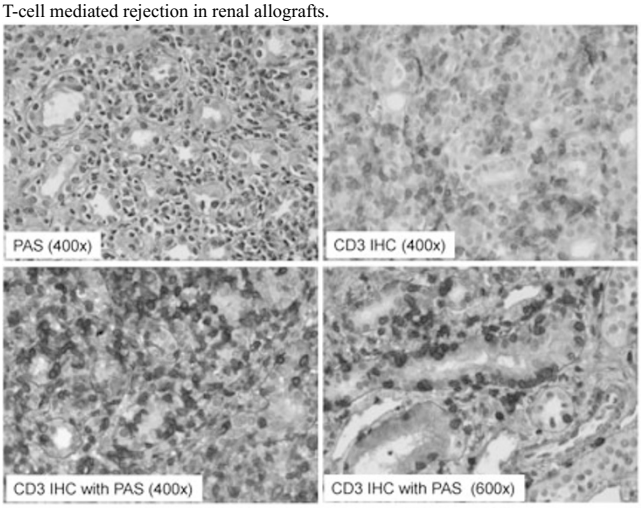

Figure 1: T-cell-mediated renal transplant rejection, Banff 1b. Comparison of tissue stained with PAS alone, CD3 IHC alone, and combined CD3 IHC with PAS.

Conclusions: This new method has greatly facilitated our work in pathological evaluation of renal transplant biopsy. We think this method is easy to perform and has a great potential to be adapted in daily practice for renal transplant biopsy evaluation.

1712 Influence of Functionally Active Plasma Cells in Acute Cellular Rejection in Renal Allografts

X Zeng, D Shi, S Sethi, M Doshi, Z Bhat. Wayne State University, Detroit, MI.

Background: Acute rejection (AR) includes T-cell mediated and antibody mediated rejection. Under light microscopy, the inflammatory infiltrate is comprised of not only T-Cells, but also varying amount of B cells (CD20+) and plasma cells (CD138+). The latter are associated with anti-body mediated rejection, which has shown poor clinical outcomes following current treatment regimens. However, the function status of these B cells/plasma cells, i.e. active antibody production, is not very clear. The phosphorylation of S6 rebosomal protein (P-S6RP) is present in cells that are metabolically active, thus identifying functional active antibody secreting plasma cells. This study is designed to evaluate the clinical significance of functional active P-S6RP plasma cells in acute rejection in renal allografts.

Design: Renal allografts with biopsy proven AR in the Detroit Medical Center during 2006-2009 were included this study. Immunohistochemistry staining for CD20, CD138 and P-S6RP was performed on paraffin slides. Renal cortex in the areas of greatest involvement is semi-quantitatively scored as 0-6. Response to anti-rejection treatment is assessed by the percentage change of serum creatinine (PC-Cr) to baseline at rejection episode (time 0) and following treatment (4 & 12 wks). Patients with lower scores (0-2) were compared to a higher scored group (3-6). The T-test for equality of means was conducted using statistical significance of $P<0.05$. C4D scores were also collected and correlate to P-s6rp, CD20 and CD138 scores.

Results: A total of 28 patients (40.7 ± 14.3 ys, M:F=15:13) were diagnosed with AR (I and II) during the study time frame. The higher scored P-s6rp group had significantly higher PC-Cr ($p<.05$) compared to the lower scored group at time 0, 4 & 12 wks following treatment, indicating poor response to treatment.

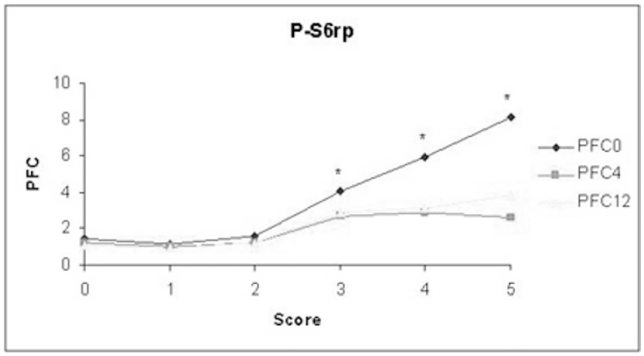

There is no significant ($P>.05$) difference in PC-Cr between higher and lower CD20 or CD138 groups. C4D scores are poorly correlated to P-S6RP, CD20 and CD138 scores.

Conclusions: The present study demonstates that the functional antibody secreting P-S6RP plasma cells are actively participating in acute rejection and are associated with poor response to treatment in renal allografts.

1713 Sox9 Staining Detects Focal-Segmental Glomerulosclerosis (FSGS) in Pediatric Steroid Resistant Nephrotic Syndrome

X Zeng. Wayne State University, Detroit, MI.

Background: In addition to minimal change disease (MCD), FSGS is an important cause of steroid resistant nephrotic syndrome in children. Under light microscopy, identification of segmental sclerosis in glomerular capillary tuft is required for the diagnosis of FSGS. Because of the "focal" nature of FSGS, the segmental sclerosis may be missed by sampling issue, therefore the diagnosis of FSGS can not be made. In addition, no reliable molecular marker for detecting FSGS is available currently. Increasing evidence indicates that FSGS is due to an irreversible podocyte damage by activation of TGF-ß mediated apoptosis and then fibrogenesis, resulting sclerosis. Sox9 is a transcriptional factor and one of the downstream targets of TGF-ß. Recent studies have been showed that Sox9 staining is positive in FSGS, but negative in MCD. Thus Sox9 can be served as a fibrogenesis marker for detecting FSGS. The purpose of this study is to evaluate the diagnostic value of Sox9 in distinguishing FSGS from MCD.

Design: Pediatric patients who had "paired-biospy", i.e. an initial biopsy with diagnosis of "MCD" then a follow-up biopsy due to sterioid resistant nephrotic syndrome with diagnosis of FSGS/MCD in Children's Hospital of Michigan during 2004-2010 were included in present study. Immunohistochemistry staining for Sox9 was performed in paraffin slide in each case. Sox9 staining (nuclear staining) in parietal epithelial cells (PEC) and podocytes were recorded as positive or negative.

Results: Seven patients had been done "paired-biopsy" in the study time frame and 4 patients had available tissue for performing immunostaining. Neither PEC nor podocyte showed Sox9 staining in initial biospy for all patients. In follow-up biospy, the Sox9 staining in podocyte is positive in FSGS patients (2/2, 100%) but negative in MCD. Sox9 staining in PEC is not detected in FSGS and MCD patient.

		1st Bx		2nd Bx	
		Podo	PEC	Podo	PEC
MCD	Case1	0	0	0	0
	Case2	0	0	0	0
FSGS	Case3	0	0	+	0
	Case4	0	0	+	0

Conclusions: Our data indicate Sox9 staining in podocyte is valuable for evaluation of evolving MCD to FSGS and may be a useful marker to distinguishing early FSGS from MCD. Study in more cases are required to confirm the present findings.

1714 Upregulated mTOR Pathway in Primary Crescentic Glomerulonephritis

PL Zhang, F Dumber, MT Rooney, W Li. William Beaumont Hospital, Royal Oak, MI.

Background: The current treatment for crescentic glomerulonephritis (CGN) is limited. The mammalian target of rapamycin (mTOR) pathway, as a major branch of growth factor-related cellular proliferation pathways, is involved in the metabolism of glomerular visceral and parietal epithelium of glomeruli in animal studies. We therefore investigated the expression of phosphorylated (p)-mTOR (activated form) and its major downstream signal p-p70S6K in CGN.

Design: The study materials included 15 unremarkable control kidney sections (removed for renal tumors), 15 samples with focal segmental glomerulosclerosis, 16 with immune complex mediated glomerulopathy (membranous GN, lupus nephritis and membranoproliferative GN) and 25 primary CGN (either ANCA associated pauci-immune type or anti-GBM type). All sections were stained for p-mTOR (Ser 2448) and p-p70S6K (Thr 389) (from Cell Signaling Technology), using a Dako Autostainer.

Results: p-mTOR and p-p70S6K demonstrated significant upregulation in renal tubules, parietal and visceral epithelium of glomeruli in all three disease groups, comparing to the control group. Serum creatinine levels in the crescentic group was significantly higher than in the other three groups. In the crescentic group, mean crescentic involvement in

glomeruli was 53.3%. A total of 22 out of 25 (88%) CGN showed upregulated nuclear staining of p-p70S6K and cytoplasmic staining of p-mTOR in the crescentic epithelium (panels B and D; arrows point to crescents), when compared to controls (panels A and C).

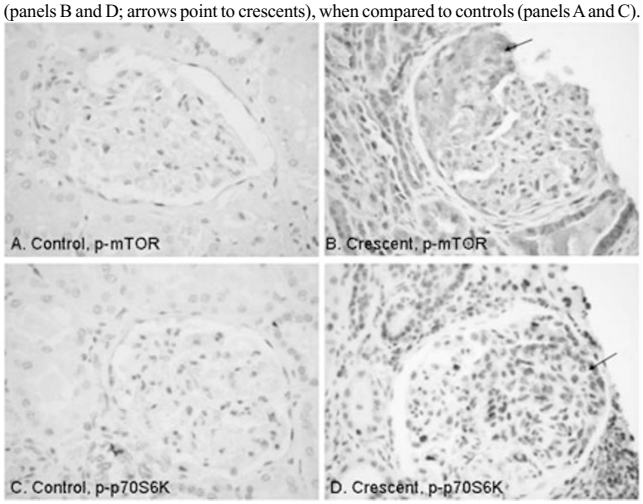

The 3 negative stained cases included 1 with fibrocellular crescents, 1 without crescents in deep sections, and 1 without glomeruli in the deep section. On PAS stained sections, upregulated unclear p-p70S6K was further confirmed in the cellular crescents.

Conclusions: In renal biopsies with various kidney diseases, a prominent upregulation of mTOR pathway signals in glomerular visceral/parietal epithelium and renal tubular epithelium was observed in all glomerulonephritis cases, indicating an increased proliferative activity in many types of glomerulonephritis. Upregulated p-mTOR and p-p70S6K in the crescentic components raise the possibility of using mTOR inhibitors as an alterative treatment in CGN.

1715 Stem/Progenitor Cell Marker CD133 Identifies Glomerular and Tubular Injury in Human Renal Biopsies

PL Zhang, MT Rooney, SK Hicks, W Li, GA Herrera. William Beaumont Hospital, Royal Oak, MI; Bostwick Laboratories, Orlando, FL.

Background: CD133, a stem/progenitor cell marker, expresses in parietal epithelial cells (PEC) of normal glomeruli and crescentic glomerulonephritis by immunofluorescent methods. This study was to investigate immunohistochemical (IHC) expression of CD133 in glomerular and tubules injury from renal biopsies.

Design: There were 16 control unremarkable renal sections (from nephrectomy for renal tumors). The acute kidney injury (AKI) group was composed of 63 native renal biopsies, with 9 primary acute tubular necrosis (ATN), 5 tubulointerstitial disease, 13 primary crescentic glomerulonephritis (GN), 14 thrombotic microangiopathy, 9 collapsing GN/HIV nephropathy, 6 biopsies with variants of monoclonal light chain nephropathy and 8 pediatric renal biopsies. They were all immunohistochemically stained for CD133 (monoclonal AC133 antibody at 1:50 dilution and a polyclonal CD133 antibody 1:500).

Results: Stains using two types of CD133 antibodies demonstrated a similar pattern of staining in normal and injured renal tissue. CD133 staining in normal PEC and crescents was confirmed as reported. In the normal kidney, there was minimal or rare CD133 staining in tubular epithelium. But in the injured proximal tubules, a gradient CD133 expression along luminal membranes was present from 1+ to 3+ (63 out of 63 cases), depending on the extent of injury. With AKI, many distal-nephron tubular cells expressed CD133 along luminal membranes as well. Double stains for CD133 (brown membranous stain) and p53 (pink nuclear stain) showed co-expression in injured renal tubules (Panel B), when compared to control (Panel A).

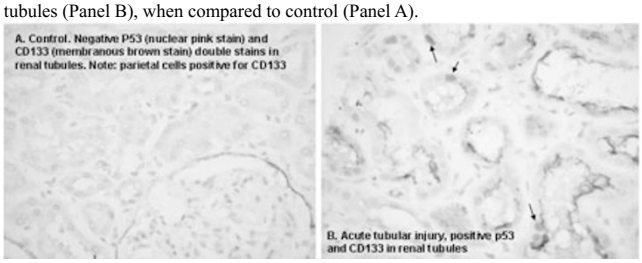

Furthermore, the tubular expression of CD133 was significantly correlated with serum creatinine levels.

Conclusions: We confirmed CD133 expression in normal PEC and crescents of CGN as shown previously. Importantly, the tubular upregulation of CD133 along luminal membranes implies that renal "progenitor-like" cells exist along tubular epithelium for tubular regeneration and the tubular injury can significantly contribute to AKI even in conventional "glomerular disorders". Finally, the IHC staining for CD133 can be used for confirming lesions in glomeruli and renal tubules of renal biopsies, better than any marker we tested.

1716 Beneficial Effects of Exogenous Thymosin ß4 on Late Stage Tubulointerstitial Fibrosis

Y Zuo, B Chun, H-C Yang, L-j Ma, AB Fogo. Vanderbilt University, Nashville, TN.

Background: Previously we showed that thymosin β4 (Tβ4), a G-actin sequestering protein, is remarkably increased in the obstructed kidney in the unilateral ureteral obstruction (UUO) model of tubulointerstitial fibrosis. Ac-SDKP, the degradation product of Tβ4 generated by prolyl oligopeptidase (POP), has anti-fibrotic effects. Moreover, we found that inhibition of POP increased Tβ4 levels, decreased Ac-SDKP levels, and exacerbated the early stage of fibrosis in obstructed kidneys. We have now investigated the long-term effects of thymosin β4 on fibrosis.

Design: Male C57BL/6 mice underwent UUO with treatments as follows, and were sacrificed at day 14: UUO without treatment, UUO+Tβ4 (150μg, i.p. q 3 d), UUO+combination (POP inhibitor, S17092, 40mg/kg/d, by gavage and Tβ4), and UUO+Ac-SDKP (1.6 mg/kg/d, delivered by minipump).

Results: Tubulointerstitial fibrosis assessed by Sirius red morphometric analysis was significantly higher in mice treated with POP inhibitor+Tβ4 combination compared to untreated UUO (3.37±0.21 vs. 2.92±0.09%, $p < 0.05$). Fibrosis was dramatically reduced by Ac-SDKP, and surprisingly, also by Tβ4 alone (Ac-SDKP 2.56±0.13; Tβ4 1.90±0.04%, both $p<0.05$ vs. untreated). We next examined POP enzyme activity and Ac-SDKP levels in the obstructed kidneys. POP activity was significantly decreased in the UUO kidneys of mice with combination treatment compared to untreated UUO kidneys (29% of levels in untreated UUO, $p<0.05$). Neither Ac-SDKP nor Tβ4 administration changed POP activity. Ac-SDKP concentration was significantly reduced by combination treatment, but was dramatically increased by Ac-SDKP or Tβ4 administration vs. untreated UUO (combination, 51%; Ac-SDKP, 199%; Tβ4, 149% of untreated UUO, all $p<0.05$ in treated vs. untreated).

Conclusions: Our study suggests that long-term exogenous Tβ4 administration may have net anti-fibrotic effects in UUO kidneys. The data demonstrate that this beneficial effect could be due to the combined actions of Tβ4 and its downstream product, Ac-SDKP. The potential beneficial effects of Tβ4 need further investigation.

Liver

1717 Fatty Liver Contributes to Hepatocarcinogenesis in Non-Cirrhotic Livers

J Alexander, M Torbenson, T-T Wu, S Kakar, D Jain, M Yeh. Univ Washington, Seattle; Johns Hopkins Univ, Baltimore; Mayo Clinic, Rochester; Univ California, San Francisco; Yale Univ, New Haven.

Background: While many specific etiologies of hepatocellular carcinoma (HCC) are well known, such as viral hepatitis and cirrhosis, the exact mechanisms of hepatocarcinogenesis remain unclear, particularly in non-cirrhotic livers. Diabetes and obesity have been established as independent risk factors for HCC. Oxidative stress has also been suggested in carcinogenesis. As steatosis is a common hepatic manifestation of these conditions, we studied the prevalence of hepatic steatosis in non-cirrhotic livers with HCC.

Design: All resected HCC cases arising in non-cirrhotic livers from 2001-2010 in 3 tertiary centers in US were searched. All resected cholangiocarcinoma (CC) cases in non-cirrhotic livers from 2001-2010 were used as control. After excluding all etiologies such as hepatitis B and/or C, hemochromatosis, α-1 antitrypsin deficiency, liver adenoma, etc, there were 157 HCC and 120 CC cases. Slides of liver distant from tumor were reviewed and steatosis was scored according to NASH-CRN. Tumor slides were reviewed in a subset of cases. Clinical data including metabolic profile were collated.

Results: As shown in the Table, the prevalence of significant steatosis (at least grade 1) in non-tumor (NT) liver in 85/157 (54%) HCC cases was greater than in 32/120 (26%) CC cases ($p<0.0001$). NT hepatic steatosis was associated with obesity ($p=0.003$) in HCC and with obesity ($p=0.002$) and diabetes ($p=0.04$) in CC. NT steatosis was associated with obesity ($p<0.0001$) and diabetes ($p=0.006$) in HCC and CC cases altogether. NT steatosis was not associated with age or alcohol use. In 40 HCC cases with tumor slides available, 18 showed the recently described steatohepatitic(SH)-HCC morphology, in which 16 had significant steatosis in NT liver, while 11 of the 22 without SH-HCC pattern had significant steatosis in NT liver ($p=0.016$). NT steatosis was not associated with steatosis in HCC.

Grade of steatosis in non-tumor liver

	0	1	2	3
HCC (n=157)	72 (46%)	56 (36%)	22 (14%)	7 (4%)
CC (n=120)	88 (73%)	21 (17%)	10 (8%)	1 (1%)

Conclusions: The prevalence of steatosis in NT liver was higher in HCC than in CC. The latter is similar to the general US population with hepatic steatosis. Obesity and diabetes were associated with hepatic steatosis in both HCC and CC. Hepatic steatosis was also associated with SH-HCC morphology. This multi-center and large cohort study underlines the role of hepatic steatosis and metabolic syndrome in hepatocarcinogenesis in non-cirrhotic liver.

1718 Pathological Characteristics of the Livers of Patients with Itai-Itai Disease (Chronic Cadmium Toxicity)

H Baba, M Yazaki, T Minamisaka, K Nagata, T Tsuda, K Tsuneyama, K Aoshima. University of Toyama, Toyama, Japan; Hagino Hospital, Toyama, Japan.

Background: Itai-itai disease (IID), which is recognized in Japan as a pollution-related illness, is caused by chronic exposure to the mineral cadmium (Cd). Excess Cd accumulation in the renal proximal tubules causes renal atrophy and secondary osteomalacia. Liver failure is a well-known complication of acute Cd toxicity, but